(NASA-CR-120706) MAN-SYSTEMS EVALUATION OF MOVING BASE VEHICLE SIMULATION MOTION CUES (Essex Corp.) 113 p HC $5.25 CSCL 05E

N75-21030

Unclas
G3/54 18154

ESSEX

ESSEX CORPORATION • 303 Cameron Street, Alexandria, Virginia 22314 •

MAN-SYSTEMS EVALUATION OF MOVING BASE VEHICLE SIMULATION MOTION CUES

Prepared by:

Mark Kirkpatrick, Ph.D.
Ronald G. Brye

ESSEX CORPORATION
303 Cameron Street
Alexandria, Virginia 22314

ESSEX CORPORATION
Huntsville Operations
11309-E South Memorial Parkway
Huntsville, Alabama 35803

Prepared for:

NATIONAL AERONAUTICS & SPACE ADMINISTRATION
Marshall Space Flight Center
Huntsville, Alabama 35812
(Under Contract NAS8-29914)

April 1974

ACKNOWLEDGEMENTS

The motion cue investigation program described in this report was formulated and performed through a joint effort by NASA MSFC Computation Laboratory and Essex Corporation. The Essex effort was performed under Contract NAS8-29914 with Mr. Frank L. Vinz of the Computation Laboratory as C.O.R.

This program would not have been possible without the support and contributions of the many MSFC Computation Laboratory personnel involved. Their dedication, interest, and technical knowledge contributed significantly to the success of the overall program.

Particular and special appreciation must go to Mr. Jim Buckner of Computer Sciences Corporation, Computer Systems and Simulation Operations Branch, Computation Laboratory for his outstanding contribution to the technical success of this program. The special efforts of Mr. Jim Young and Mr. Oscar Hobson of Hayes International Corporation, Communications Branch and Mr. John Archambeoult, Link Representative must be noted here for their invaluable support in maintaining the program equipment and providing technical assistance to every phase of the program.

The technical advice and coordination provided throughout the program by Mr. Frank L. Vinz as C.O.R. and by Mr. Maurice H. Knighton, NASA engineer, were extremely helpful and greatly appreciated.

Special thanks must be given to the many people who participated as test subjects in this program who gave up considerable time and energy towards making this a successful experimental program and their good humor, patience, and interest were appreciated throughout the program. Thanks are owed to Ms. Elizabeth Esch for her typing the final manuscript and to Mr. Sheldon Shenk for his graphics work.

SYMBOLS

$\Delta V/\Delta T$	Linear acceleration parameter for velocity ramp
X	Fore-aft motion axis
Z	Vertical motion axis
θ	Pitch axis (rotation about the Y axis)
Y	Right-left motion axis
DOF	Number of unconstrained axes of a physical system
g	Acceleration due to gravity at sea level
df	Statistical degrees-of-freedom - corrected sample size which produces unbiased statistical estimation
SS	Sum-of-squares - the sum of squared deviation of a set of sample values about their mean
MS	Mean square or variance - the unbiased estimate of the mean squared deviation of a set of sample values about their mean
F	F-ratio - a hypothesis testing statistic found by the ratio of two mean squares
a	Absolute linear acceleration value $a = \lvert\ddot{X}\rvert$ or $\lvert\ddot{Z}\rvert$
T	ΔT Interval Duration
D_x	Derived detectability figure of merit for accelerations along the X axis
D_z	Derived detectability figure of merit for accelerations along the Z axis
e	Base of natural logarithms
P	Forced-choice detection probability
b	Free parameter used in regression equations for P on D_x, D_z, or D_θ
A	$\log e \frac{1-P}{.5}$
$\underset{\sim}{b}$	Estimate of b

α	Absolute angular acceleration value $\alpha = \lvert\ddot{\theta}\rvert$
D_θ	Derived detectability figure of merit for angular accelerations in the pitch axis
W^2	Proportion of total variance of P which is due to individual differences in acceleration sensitivity
V_M	Maximum velocity during test interval
d	Total distance travelled
E	Error of estimation for a single data point
$\bar{\ }$	Bar indicates the mean of the variable over which it is placed

TABLE OF CONTENTS

TABLE OF CONTENTS, Continued:

TABLE OF CONTENTS, Continued:

TABLE OF CONTENTS, Continued:

TABLE OF CONTENTS, Continued:

TABLE OF CONTENTS, Continued:

Section | Page

List of Tables

TABLE OF CONTENTS, Continued:

1.0 INTRODUCTION

The study reported here deals with human factors aspects of high fidelity vehicle simulation. To adequately simulate a surface, air, or space vehicle with the operator in the loop requires that vehicle motions in six degrees of freedom be adequately represented as the operator outputs command and control actions. This entails reproducing position and its first two derivatives in six degrees of freedom via the simulation apparatus.

The problem is that while a six degree of freedom simulator can be constructed, the structural details will constrain the cab to certain travel excursions in each axis. While acceleration characteristics of the vehicle in question can be produced depending on cab/structural mass and driving force, the resulting rates cannot be maintained indefinitely due to travel limits in all six axes.

These limitations on cab travel for any given simulator thus place a restraint on the fidelity in terms of actual motion which can be presented to the operator. A theoretical approach to the solution of the problem rests on the nature of the human response to non-visual motion cues. Assuming that the simulation technique involves a cab-mounted visual display system (as opposed to external projection) then the problem becomes one of producing cab motions which approximate the real vehicle motion with an error not detectable by the motion sensing capabilities of the operator. This approach involves commanding an "onset" cab acceleration which represents the initial acceleration profile of the actual vehicle and then nulling this acceleration. The real vehicle might maintain this acceleration and resulting velocity but the simulator cab cannot due to travel constraints. Therefore, the cab must

be brought to rest at a deceleration not perceptible to the operator. It should also be returned to a central position on the axis in question so that the system may respond to further operator commands. Such a procedure is generally referred to as a "washout technique". Its use depends on the demonstrated fact that the human sensory system does not directly sense velocity other than visually and that the response to acceleration via the vestibular system, limb position, pressure sensing, etc. presumably exhibits a threshold effect, acceleration below some value producing a negligible probability of detection by the operator.

The values of this threshold for the various axes should thus serve as upper limits on accelerations produced by the "washout technique" in order to prevent spurious cues due to the simulator itself. The threshold values thus constrain the maximum acceleration which can be used during "washout".

The application of washout techniques to vehicle simulation is a topic of considerable current interest to those involved in complex simulation as attested by the fact that a recent conference on simulation at NASA's Ames Research Center included papers dealing specifically with washout methodology (Refs. 1,2). The interest in washout techniques reflects the increasing sophistication of simulation in recent years - particularly in the pilot training and pilot performance research areas. Lack of fidelity of motion cues impacts the validity of obtained results from simulators in at least two ways. The existence of spurious cues specific to the simulator may elicit invalid responses from the experienced pilot. In the case of pilot training, they may contribute to "learning to fly the simulator" as opposed to learning skills which will readily transfer to the real aircraft situation. A second effect is that spurious cues presumably contribute to motion disturbance experienced by many subjects in simulation programs. Much of this difficulty

is thought to derive from the fact that the motions of most real vehicles result in correlations or dependencies between the visual and vestibular cues experienced by their passengers. With enough experience on the real system, spurious cues would then disturb the normal learned correlations when an experienced operator is exposed to simulation of the vehicle in question.

The investigation described here was conducted using the General Purpose Simulator at NASA's Marshall Space Flight Center. This facility is a six degree of freedom moving base simulator designed to simulate a wide range of vehicles. Studies conducted using the device have dealt with aerodynamic vehicles, lunar surface vehicles, and surface effects ships. Some of the state-of-the-art features of the MSFC general purpose simulator include:

- Wide angle vision system (136 x 42 degrees)
- Color visual presentation
- Articulated Scheimpflug camera probe having infinite depth-of-field and roll, pitch, & yaw rotations
- Virtual image projection
- 40 x 15 ft (12.2 x 4.6 m.) terrain model
- 3 degree-of-freedom camera gantry
- 6 degree-of-freedom motion base
  - translation up to $\pm$ 4 ft (1.2 m.)
  - attitude up to $\pm$ 32 degrees

The current study employed the General Purpose Simulator to study motion cue thresholds in three axes - fore/aft translation, vertical translation, and pitch. The study was part of an effort to provide adequate fidelity to employ the simulator in investigations of various vehicles including:

- Automobiles and other high vehicles
- Surface effect vehicles
- Public transportation vehicles
- Fixed and rotary wing aircraft
- STOL, VTOL, VSTOL aircraft
- Commercial aircraft
- Orbital vehicles

The study conducted here had two purposes - to provide further general data on non-visual motion thresholds and to establish specific threshold values for use as washout parameters in vehicle simulation using the MSFC General Purpose Simulator. Thus, the data reported serve both a specific technology development and a general research function.

A preliminary review of the available data on translation and attitude acceleration thresholds disclosed considerable variation in results. Some of these results have been summarized by Huddleston (Ref. 3). A list of selected threshold results appears in Table 1-1 partly taken from Huddleston and partly from other sources.

Several possible explanations for the observed variation in results may be put forth. These generally may be classified as differences between subjects and differences in methods used by various investigators. Stewart (Ref. 11) has stressed the individual differences between subjects in acceleration sensitivity and Clark and Stewart (Ref. 12) have presented data on yaw thresholds suggesting a range from .10 to 3.20 degrees/sec^2 for the between-subject distribution using a detection response method. Use of the oculogyral illusion was found to yield a smaller range of from .01 to .60 degrees/sec^2. While these data clearly indicate substantial differences between subjects in terms of acceleration sensitivity, differences in method also exist.

The greater sensitivity of the oculogyral illusion as opposed to dectection response methods is well illustrated in the work of Stewart (Ref. 11) and Clark and Stewart (Ref. 12). There is reason also to suppose that the response method used for detection responses may influence results. The argument for the method of forced choice is discussed in Appendix I. It will suffice to note here that recognition of the bias effects or decision process on the part of observers as a strong factor in threshold measurement and the development

TABLE 1-1 SUMMARY OF THRESHOLD DATA

AXIS	THRESHOLD			REFERENCE
X	12.0 - 20.0	cm / sec^2		(4)
	20.0 - 80.0	cm / sec^2		(5)
Y	1.0 - 3.0	cm / sec^2		(6)
	12.0 - 20.0	cm / sec^2		(4)
Z	1.7 - 4.0	cm / sec^2		(7)
	1.0 - 5.0	cm / sec^2		(6)
	4.0 - 12.0	cm / sec^2		(4)
	6.0 - 15.0	cm / sec^2		(8)
	4.9	cm / sec^2		(9)
Pitch	4.0	deg/ sec^2	(impulse velocity)	(10)
	.67	deg/ sec^2	(detection response)	(10)
Roll	4.0	deg/ sec^2	(impulse velocity)	(10)
	.41	deg/ sec^2	(detection response)	(11)
Yaw	4.0	deg/ sec^2	(impulse velocity)	(10)
	.05- 2.2	deg/ sec^2	(detection response)	(11)
Average - Pitch, Roll, Yaw	.05- .28	deg/ sec^2	(oculogyral illusion)	(11)

of appropriate sensitivity measures has been carried out since the early 1960s. Earlier threshold studies have been questioned because of these methodological advances (Green and Swets, Ref. 13). Variability of results due to small methodological variations - even in the case of logically equivalent procedures - has been noted in earlier threshold studies for many sensory modes. For this reason, it is tenable to suppose that pre-1960 acceleration threshold studies may have produced variable results due to failure to control observer decision processes. It should be noted that the work of Stewart (Ref. 11) and Clark and Stewart (Ref. 12), however, is free of this deficiency since they employed the method of forced choice.

The purpose of the current study, then, was to establish or confirm permissible velocity change rates for specific application in washout technology for use in the MSFC General Purpose Simulator. One feature of this simulator, as noted previously, is a state-of-the-art visual system. Washout of translation or attitude rates in such a simulator involves contradictory cues since during washout, appropriate visual cues (associated with a constant rate) would be available. Since acceleration threshold studies have typically been conducted under visually impoverished conditions, the present study undertook to test the hypothesis that acceleration sensitivity would be reduced during a vehicle control task involving visual feedback as compared with a condition having the subject in darkness and emitting no control actions. Such a differential sensitivity effect would permit higher washout velocity change rates during actual vehicle simulation. To perform the study, three experiments were carried out in three selected degrees of freedom. The MSFC General Purpose Simulator was programmed to provide varying acceleration levels and the method of forced choice based on the theory of signal detectability (Green and Swets, Ref. 13) was employed.

2.0 TECHNICAL APPROACH

2.1 - General Simulation Method

The NASA Marshall Space Flight Center general purpose Six Degree-of-Freedom (6 DOF) motion simulator was programmed to execute a pre-established motion sequence for each axis under investigation. A motion sequence consisted of the base being driven in one of two directions in each of three axes (horizontal, vertical, or pitch), either accelerating or decelerating. Constant amplitudes of acceleration were combined with various time durations. Each motion sequence was presented under two different test conditions - baseline, no visual cues or secondary task, or a contradictory cue condition, a visual scene being presented at a constant forward velocity combined with a steering task of lateral motion control.

During each motion sequence the subject was presented with two test intervals and he was to decide in which interval he judged the signal (change in velocity) to be present. This decision was reported via a response panel which interfaced with a hybrid computer using two discrete sense lines. The sequence of events from initiation of motion sequence through response by the subject was termed a trial.

Four motion profiles each having various $\Delta V/\Delta T$ values combined with two directions of motion produced 40 trials. Figure 2-1 presents the four basic motion profiles used throughout the testing program.

2.2 - Event Sequence and Response Method

Each trial began with the base slowly accelerating (value lower than lowest test signal) to reach an initial velocity. This initializing permitted the subject's sensory system to adapt as well as reducing base lurches when

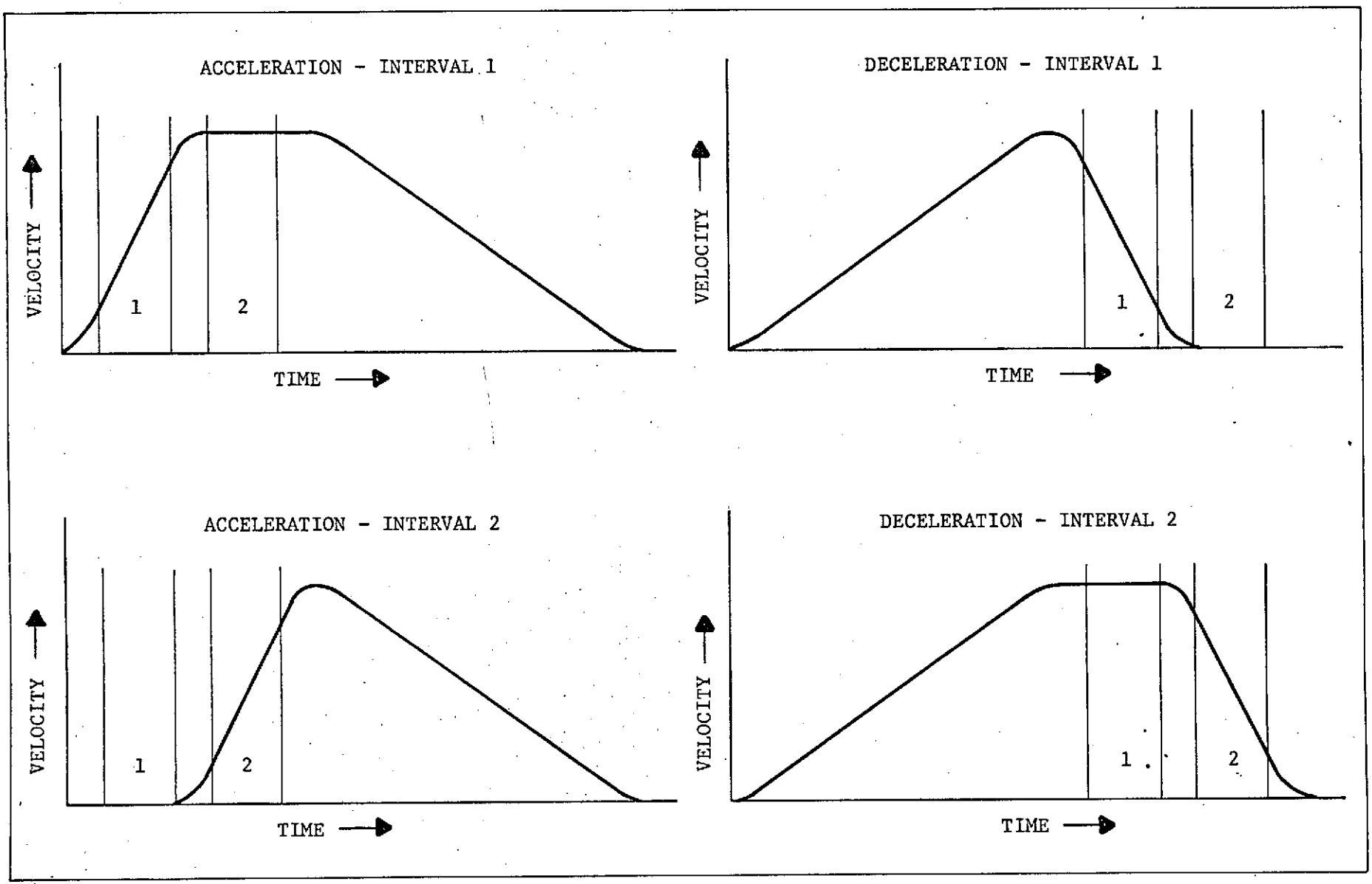

FIGURE 2-1. Velocity Profiles

velocity changes were introduced. During the initialization period a "ready" lamp lighted on the subject response panel in the cab signalling the subject that a trial was to begin. This lamp remained lit during the initialization period and then went off before test interval 1 started.

During test interval 1 a signal (velocity change) was either present or absent. A lamp on the subject response panel lighted, indicating test interval 1. This lamp remained lit during the test interval and then went off. After a short time pause, test interval 2 then began and a signal was either present or absent depending upon a signal presentation during interval 1. During this interval a lamp on the response panel was lighted signalling test interval 2. The test interval 2 lamp remained lit during the test period and then went off. After a short pause the response lamp was lighted signalling the subject to respond by throwing one of two response switches corresponding to the interval he judged the signal to be present in. The response lamp remained lit until a response was made. After completion of the response the base then recycled for the next trial and the procedure repeated.

Each trial contained only one signal assigned at random to one of the two test intervals. The digital computer tested the subject response against the true state of affairs and recorded whether the response was correct or in error.

2.3 - Axes Investigated

Three axes of motion were investigated for this program (See Figure 2-2). Experiment 1 investigated velocity-change detection in the fore-aft translational axis of motion. Experiment 2 investigated velocity-change detection in the vertical translation axis of motion. Experiment 3 investigated velocity-change detection in the pitch rotational axis of motion. In each experiment

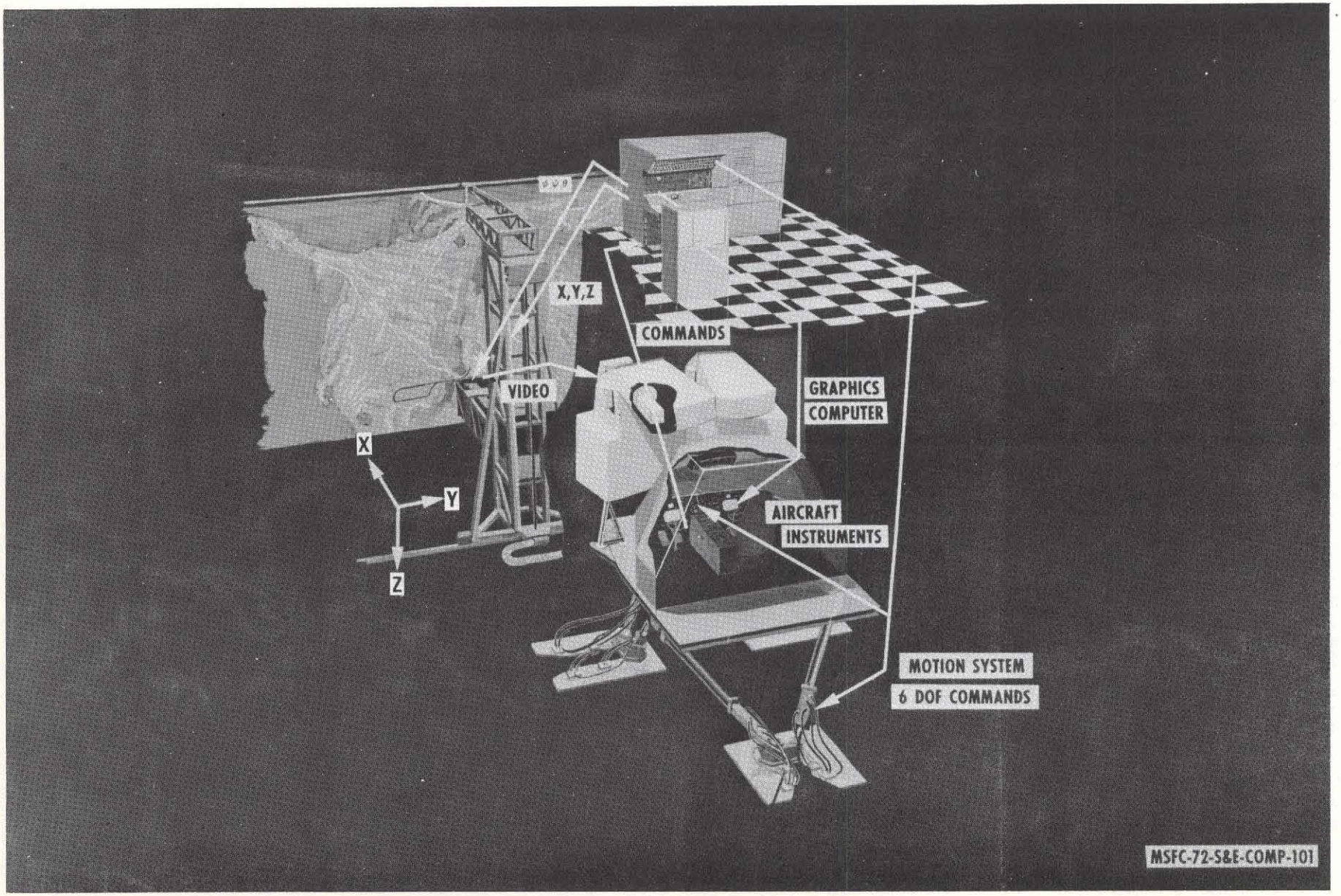

FIGURE 2-2. AXIS IDENTIFICATION

the subjects' only concern was detection of a change in velocity rather than the direction of motion.

2.4 - Simulation Apparatus

The laboratory facilities used are located in the Computation Laboratory at MSFC. Three main systems were employed throughout the testing program:

- MSFC 6 DOF general purpose motion simulator with enclosed cab and video display.
- A hybrid computer system which provided control of the motion base and data recording functions.
- An optical pickup system, TV camera, and a 15' x 40' three dimensional terrain model.

Figure 2-3 presents the block diagram for these three systems.

The MSFC Six Degree-of-Freedom moving base simulator is manufactured by the Singer Corporation and is capable of providing independent motion in six degrees of freedom by simultaneous yet discrete operation of six 5-foot hydraulic actuators arranged in three bipod pairs between the base and floor. Figure 2-4 shows a model of the General Purpose Simulator in a pitch-down configuration. Figure 2-5 shows the hydraulic actuator system. The dynamic performance capabilities of the motion system are given in Table 2-1.

The base carried a completely enclosed cab where the subject was located. Located in the cab were the subject response panel, a wide angle video display system, steering wheel, airline pilot's seat, and headphones for communication. The cab interior is shown in Figure 2-6.

The hybrid computer system consisted of an Electro-Mechanical Research 6050 digital computer and an Applied Dynamics 9800 analog computer. The digital computer provided actuator commands for positional change as a function of time (12.5 mS integration), test sequence logic (interval 1 or 2), statistical calculations, and recorded subject response.

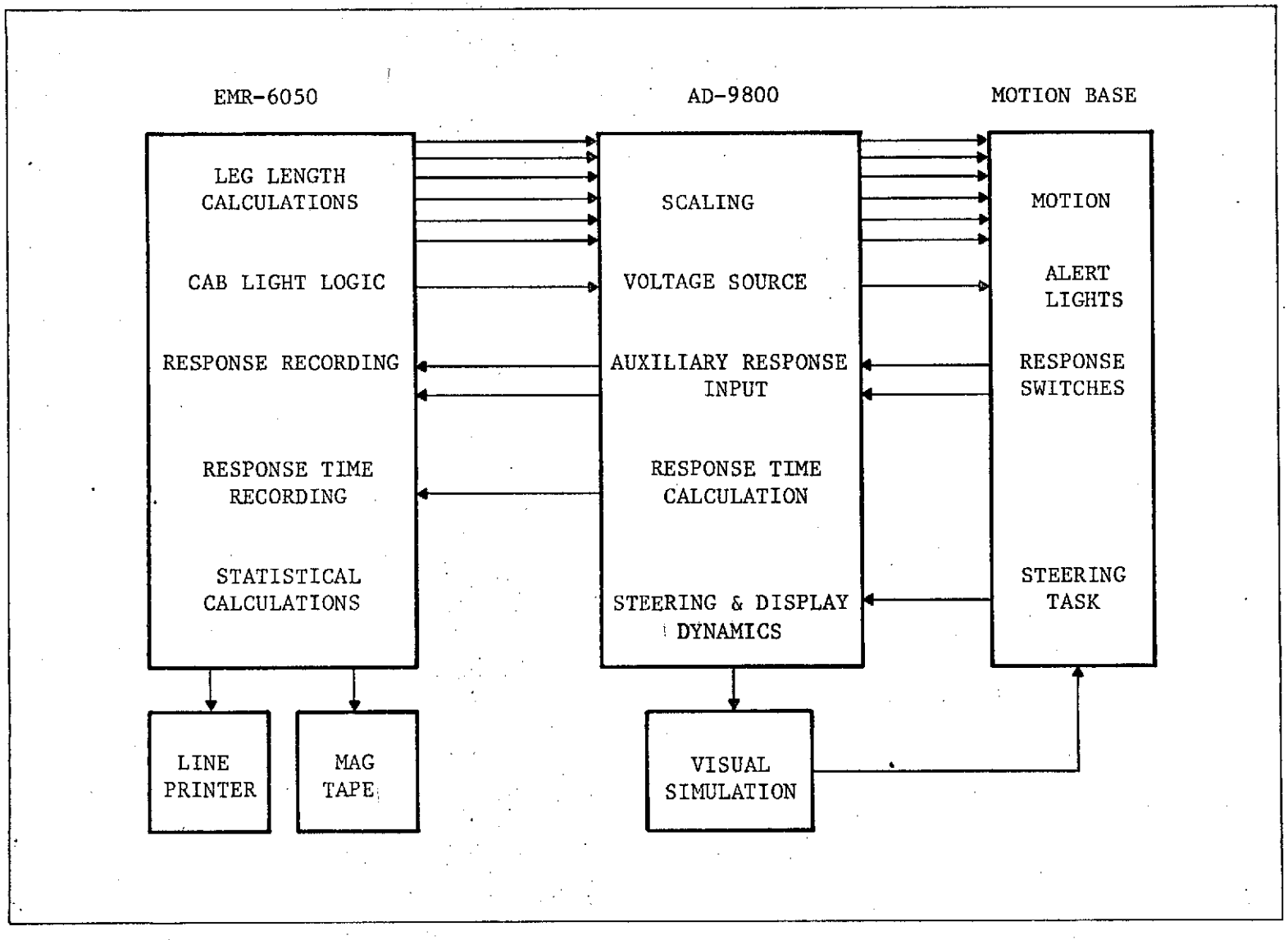

FIGURE 2-3. Simulator System Block Diagram

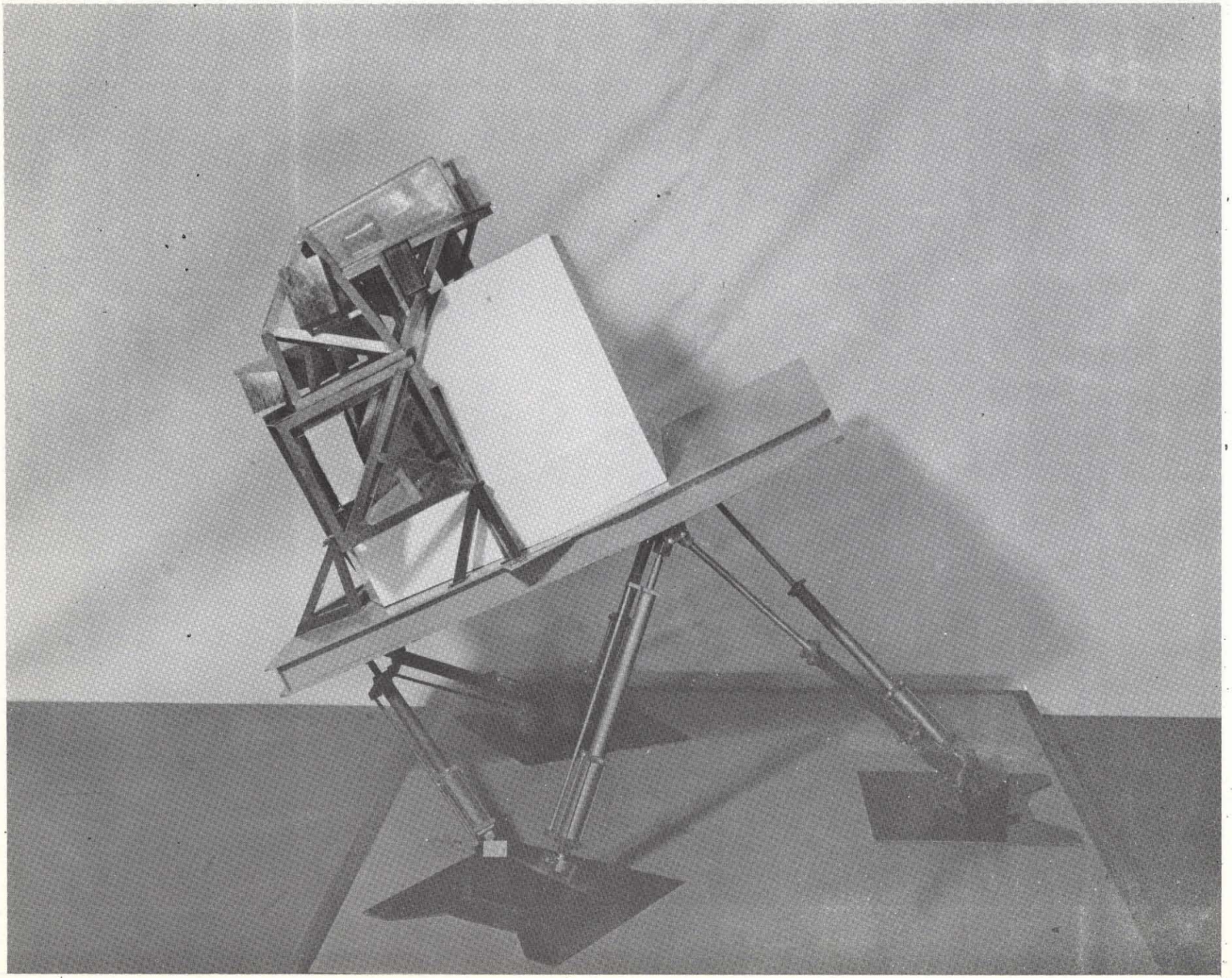

FIGURE 2-4. MSFC 6 DEGREE-OF-FREEDOM MOVING BASE SIMULATOR IN A PITCH DOWN POSITION

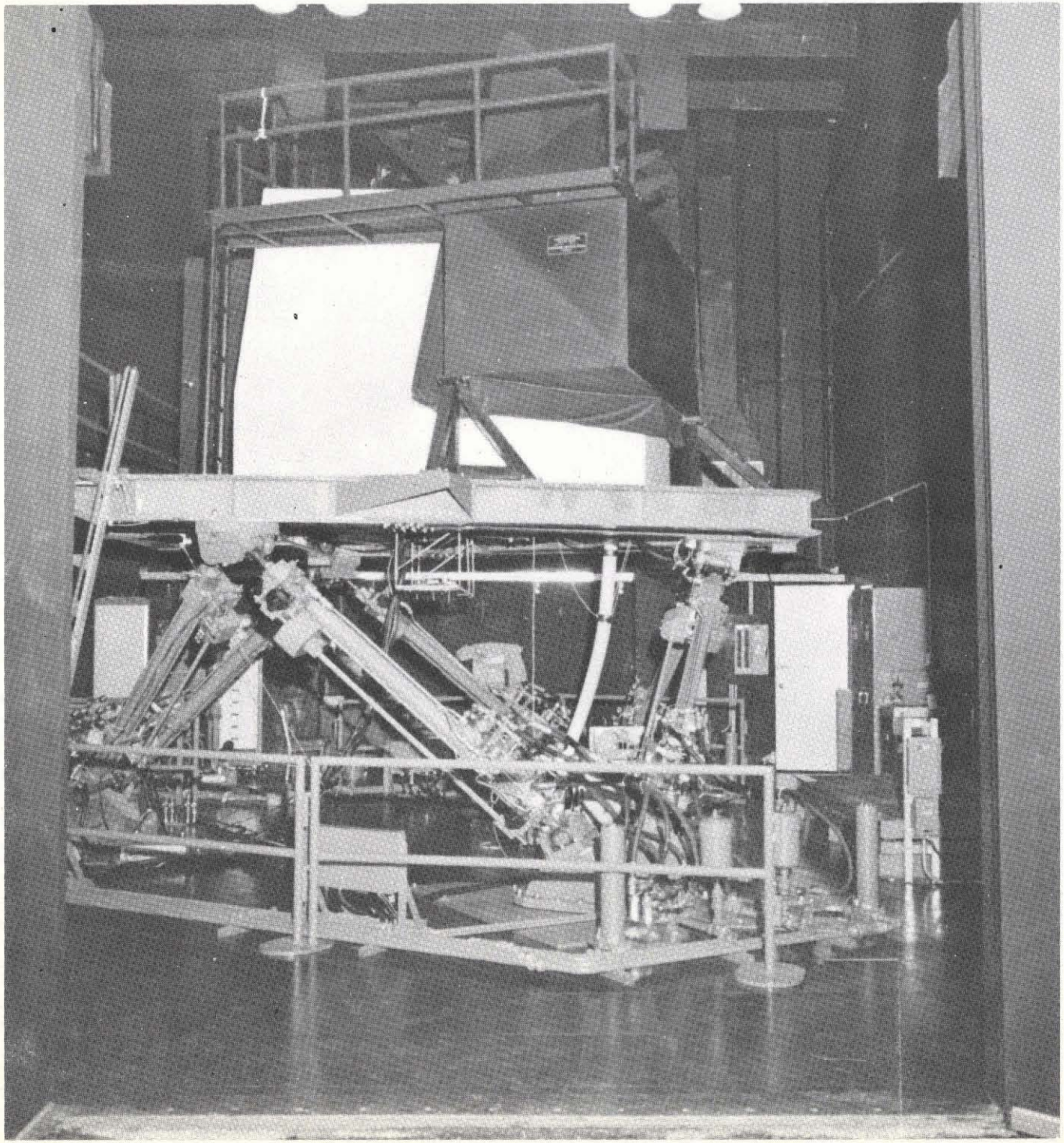

FIGURE 2-5. MOVING BASE SIMULATOR HYDRAULIC ACTUATOR SYSTEM

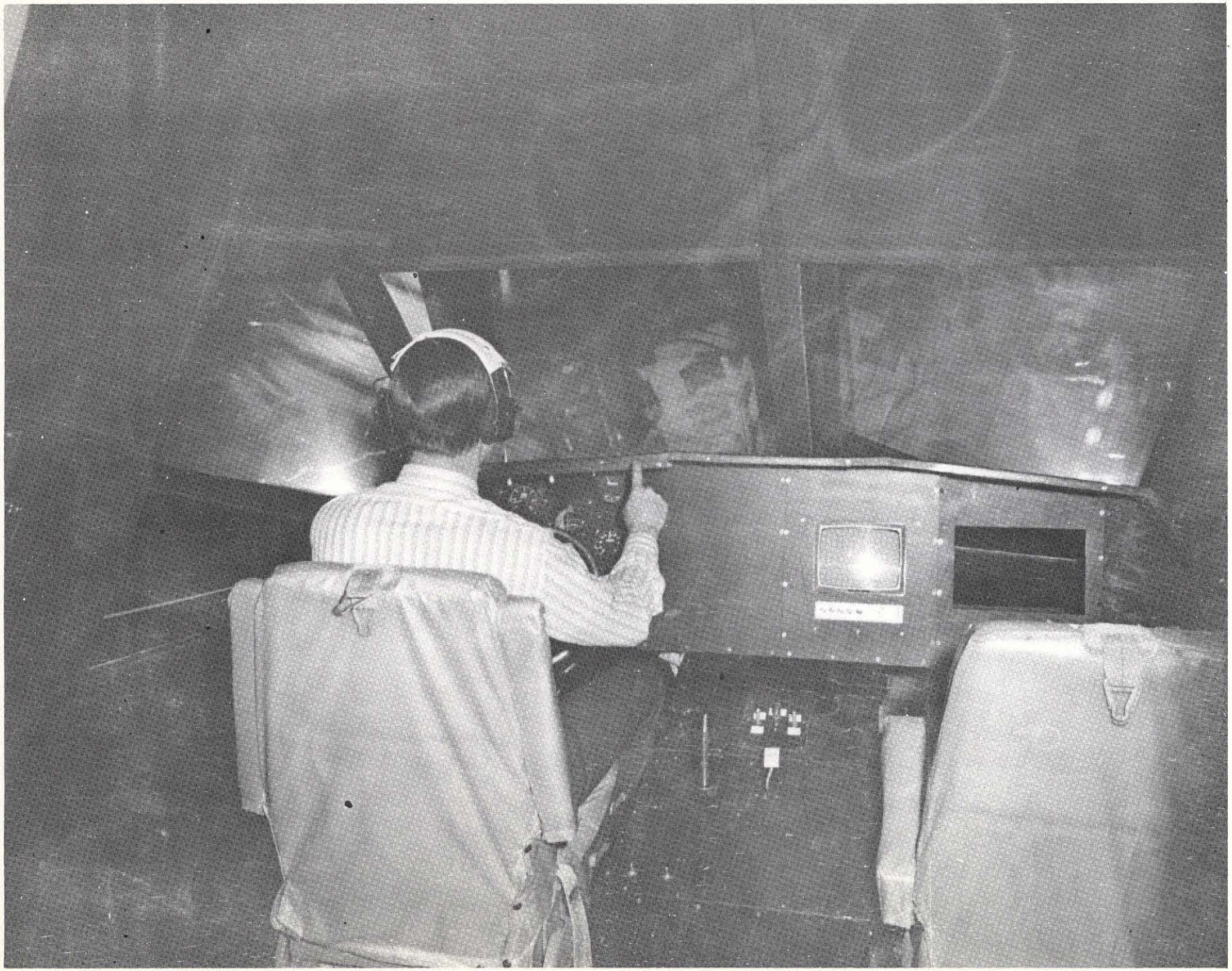

FIGURE 2-6. INTERIOR OF CAB WITH SUBJECT IN TEST POSITION

The analog computer provided trunking between the digital computer and motion system, transmitted response inputs to the digital system and provided steering and display dynamics.

Dependent data were collected on a line printer for real-time display and recorded on magnetic tape for later statistical analysis.

The optics system consisted of a Dalto Electronics Corporation DEC M-15 gantry fitted with a 140 degree Farrand optical probe having Scheimpflug infinite depth-of-field capability and a Thomson-Houston THV-170/C field sequential camera operated without the color wheel as a black and white system. The optical probe and terrain model are shown in Figure 2-7.

The DEC M-15 gantry is a servo-driven unit providing three degree-of-freedom translational motion of the optical probe and television camera along a three dimensional terrain model containing a two-lane automobile highway. The THV-170/C camera provided a 441 scan line, 180 fields per second, video format. The Farrand display is a multi-channel device having 140 degree horizontal field-of-view capability. For this study it was operated with only one camera which provided a 45° horizontal by 38° vertical image of the terrain model. Collimated projection added realism to the image by making it appear a great distance from the test subject and thus eliminating parallax effects.

2.5 - Test Subject Selection

Subjects were selected within the Computation Laboratory and screened as to history of inner ear troubles and normal vision. A total of 35 subjects participated in the program - 18 for fore-aft translation, 7 for vertical translation, and 10 for pitch rotations.

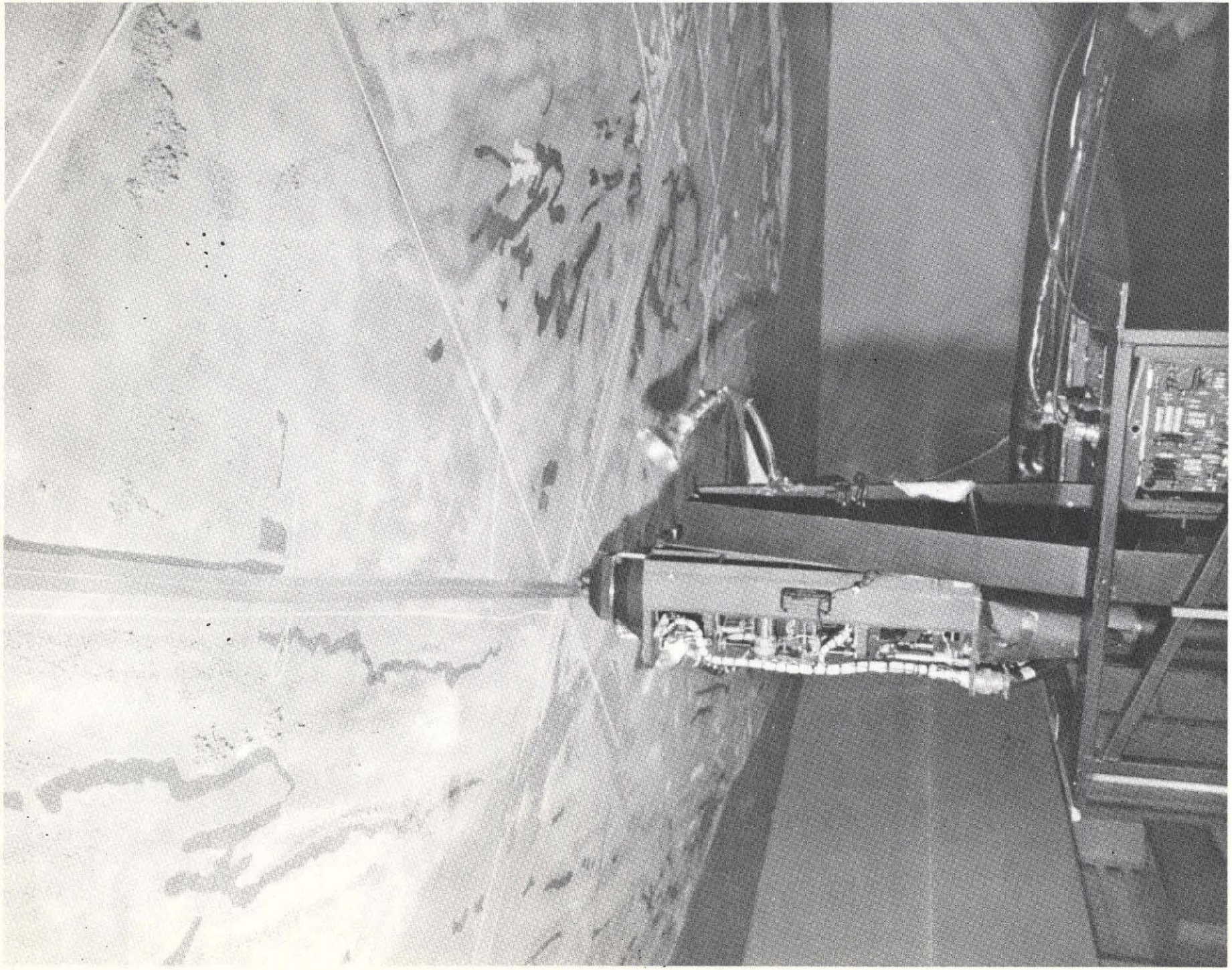

FIGURE 2-7. OPTICAL PROBE AND TERRAIN MODEL SHOWING SIMULATED TWO-LANE AUTOMOBILE HIGHWAY

2.6 - Contradictory Cues Condition

This portion of the testing program measured the impact of contradictory visual cues combined with a secondary task on the overall accuracy of signal detection as compared with that from the baseline data. As with the baseline condition each subject completed a block of 40 trials under the test condition. The block of trials presented was identical in every respect to that of the baseline with the exception the subject was given a view of a long two-lane highway and instructed to steer along this road.

The subjective sensation was that of driving along a highway with moderate crosswinds. The forward velocity was preset by the hybrid computer and could not be modified by the subject's action. His only task was to command lateral translation, or steer, by turning the steering wheel, left or right to stay within the confines of the highway and not concentrate on maintaining a fixed lane position. No data were recorded as to frequency of off-road incidents but the subject's steering performance was monitored by the experimenter and in the event of large or/and lengthy off-the-road deviations or high frequency of off-road incidents the subjects were cautioned to stay on the road. All subjects performed the steering task with few deviations.

Fixed parameters for the contradictory cues condition are presented below:

Vehicle Velocity (forward)	25 miles/hr
Steering Wheel (angular) Displacement	340^{o} (lock-to-lock)
Steering Sensitivity Ratio	60%
Steering "Noise" Ratio	3.2161 positive feedback
Time Delay Constant for "Noise" Oversteer	0.1 second

The crosswind effect was perceived as a wind pushing the vehicle in the same direction as was steered. The strength of this wind was directly related

TABLE 2-1 PERFORMANCE OF SIX-DEGREE-OF-FREEDOM MOTION SYSTEM

	Position	Rate	Acceleration
PITCH	$+30^{\circ}$, -20°	$\pm 15^{\circ}$/sec	± 6.5 rad/sec^2
ROLL	$\pm 22^{\circ}$	$\pm 15^{\circ}$/sec	± 7.0 rad/sec^2
YAW	$\pm 32^{\circ}$	$\pm 15^{\circ}$/sec	± 6.0 rad/sec^2
VERTICAL	39 in (99 cm) Up 30 in (76 cm) Down	± 24 in/sec (± 61 cm/sec)	± 1.6 g
LATERAL	± 48 in (± 122 cm)	± 24 in/sec (± 61 cm/sec)	± 2.4 g
LONGITUDINAL	± 48 in (± 122 cm)	± 24 in/sec (± 61 cm/sec)	± 2.0 g

to angular displacement of the steering wheel so that each 1^{o} change in the wheel produced a 1.5 mile/hr increase in wind. If left uncorrected, the vehicle continued to change heading - eventually going off the road. To correct for the crosswind the subject steered opposite until a change in heading was noticed, then slowly reduced the turning of the wheel until he was back on the road and headed straight. A 0.3 second delay between turning the steering wheel and noticeable change in heading provided realism to the steering task. Although the steering wheel has a $\pm 170^{o}$ capability, the average displacement during testing was about $\pm 2^{o}$.

The contradictory cue condition was not designed to represent any particular vehicle but simply to provide a visual scene showing forward motion and a control task of moderate difficulty. Since these were considered to be the primary characteristics of vehicle simulation, the present method, although arbitrary, appeared sufficient to test the general contradictory cue hypothesis.

3.0 EXPERIMENT 1 - FORE-AFT MOTION SIGNAL DETECTION

3.1 - Objective

The objective of Experiment 1 was to measure linear acceleration sensitivity in the forward-aft (± X) directions. Data were collected under baseline conditions (no visual cues) and then when contradictory cues (visual cues plus steering task) were introduced.

3.2 - Apparatus

The apparatus consisted of the six degree-of-freedom motion base and the response panel located in the cab.

Contradictory visual cues were provided via the television system described in Section 2.0. An automobile steering wheel mounted in the cab enabled the subject to command lateral translation while the hybrid-computer maintained a constant forward speed.

Communication between the experimenter and subject was provided by headphones which also helped mask auditory cues from the motion base hydraulic system which might influence subject performance.

3.3 - Experimental Design

Five independent variables were manipulated in Experiment 1. These variables and their levels were as follows:

Test Condition	Baseline (no visual cues) or contradictory (steering plus visual scene with constant forward velocity)
Direction or Motion	Forward or Aft
Velocity Change	Acceleration or Deceleration
Test Signal Duration	0.5, 1.0, or 1.5 seconds
Magnitude of Velocity Change	0.2 to 1.5 ft/sec^2 (0.006 to 0.047g)

The combinations of magnitude of velocity change and interval duration were selected based on simulator travel constraints, available literature on fore-aft acceleration sensitivity, and the results of the pilot study used to select levels for the main experiment. The ten cases employed are described in Table 3-1.

Eighteen subjects performed the tests under all combinations of levels of the independent variables. Each subject completed a block of 40 trials under one of the two test conditions, baseline or contradictory cues, before going to the next block of 40 trials. The order of presentation of specific treatment levels was randomized per block of 40 trials.

3.4 - Procedure

Baseline conditions - Each subject was instructed to adjust the seat in front of the steering wheel to where he would normally be when driving an automobile. A seat belt was then loosely fitted around the waist for protection in case of malfunctions. He was instructed to place his feet on a pad to minimize vibration and keep his hands in his lap until ready to make a response. Instructions were given to each subject as to the objective of the test, sequencing of the test panel lamps and activation of the response switches. The headphones were positioned and the noise source turned on. Each trial began with the "ready" lamp lighting, signalling a trial was to begin. This lamp went off and the test interval 1 lamp lighted. During this interval, a test signal was either present or absent. This lamp went off and test interval 2 lamp lighted. During this interval a signal was either present or absent. Interval 2 lamp went off and the response lamp lighted cueing the subject to respond by selecting interval 1 or 2 response switch. After subject response, the motion base system recycled for the next trial and the same procedure repeated.

TABLE 3-1

ABSOLUTE MAGNITUDE OF VELOCITY CHANGE AND INTERVAL DURATION FOR EXPERIMENT 1

Case	Interval Duration (sec)	Acceleration		
		g	ft/sec^2	cm/sec^2
1	.5	.006	.193	5.883
2	.5	.012	.386	11.765
3	.5	.019	.611	18.623
4	.5	.031	.997	30.389
5	.5	.047	1.512	46.086
6	1.0	.019	.611	18.623
7	1.0	.031	.997	30.389
8	1.5	.006	.193	5.883
9	1.5	.012	.386	11.765
10	1.5	.019	.611	18.623

Contradictory cue condition - This sequence of testing was identical to that of baseline, with the exception of the subject being required to steer along a two-lane road during the entire test period. Positive feedback from the steering commands gave the effect of a moderately difficult tracking task that was more demanding than ordinary driving.

The subjects were allowed practice steering along the road with no cab motion prior to actual testing. During actual testing, their only criterion for steering was that they attempt to "stay on" the road, and in most cases, the test subjects were able to do so.

3.5 - Results and Data Analyses

The dependent measure employed in Experiment 1 was signal (velocity change) detection accuracy. Signal detection was scored as being correct or incorrect based upon the test interval selected by the subject versus the test interval the signal was presented in.

These data were subjected to a five-way analysis of variance assuming a treatments by subjects design and all factors fixed except subjects. Table 3-2 presents the signal detection accuracy source table.

Table 3-2 shows the main significant sources of variance to be direction of travel, sign of velocity change, and case which refers to the $\Delta V/\Delta T$, ΔT combinations employed. The main effect of test condition was not found to reach the .05 level of significance. The data, therefore, fail to support the hypothesis of generally depressed sensitivity due to introduction of the steering task and its associated visual cues. A significant interaction ($p < .05$) was, however, obtained between test condition and direction of travel. This effect is illustrated in Figure 3-1. Figure 3-1 suggests that

TABLE 3-2

ANALYSIS OF VARIANCE OF X-AXIS
VELOCITY CHANGE DETECTION PROBABILITY

Source	df	SS	MS	F
Test Condition (T)	1	.62	.62	2.76
Direction of Travel (D)	1	2.50	2.50	16.83**
$\pm \Delta V$ (G)	1	1.88	1.88	9.41**
Case (C)	9	17.72	1.97	13.95**
Subjects (S)	17	5.92	.35	--
T x D	1	.80	.80	9.94**
T x G	1	.03	.03	.16
T x C	9	.57	.06	.53
T x S	17	3.85	.23	--
D x G	1	.10	.10	.66
D x C	9	7.69	.85	5.68**
D x S	17	2.52	.15	--
G x C	9	4.96	.55	4.43**
G x S	17	3.41	.21	--
C x S	153	21.60	.14	--
T x D x C	1	.22	.22	1.66
T x D x C	9	1.03	.11	.83
T x D x S	17	1.37	.08	--
T x G x C	9	.56	.06	.46
T x G x S	17	2.60	.15	--
T x C x S	153	18.21	.12	--
D x G x C	9	9.98	1.11	7.51**
D x G x S	17	2.57	.15	--
D x C x S	153	23.03	.15	--
G x C x S	153	19.02	.12	--
T x D x G x C	9	.27	.03	.26
T x D x G x S	17	2.30	.13	--
T x D x C x S	153	21.04	.14	--
T x G x C x S	153	20.57	.13	--
D x G x C x S	153	22.59	.15	--
T x D x G x C x S	153	17.95	.12	--
TOTAL	1439	237.50		

*Significant at the .05 level
**Significant at the .01 level

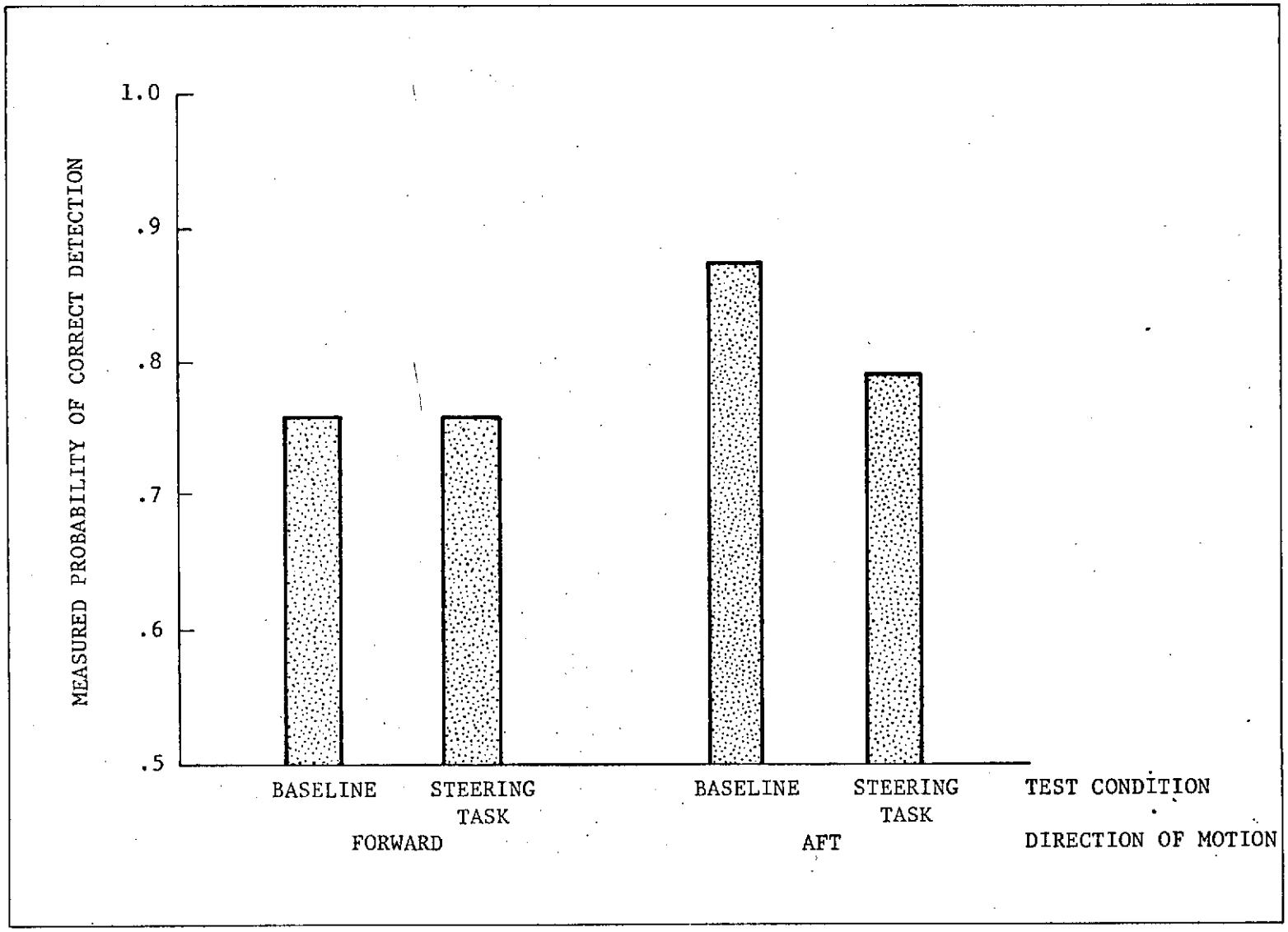

FIGURE 3-1. Measured Probability of Correct Detection of X-Axis Velocity Change as a Function of Test Condition and Motion Direction

depression of acceleration sensitivity does occur but only under motion in the aft direction. This suggests that the effect of the steering task and visual cues to forward motion may permit higher accelerations than would be expected from baseline data in returning the cab to its central position following washout but has little effect on permissible decelerations during washout.

The main effect of the sign of the velocity change is illustrated in Figure 3-2. The data suggest greater sensitivity to deceleration than to acceleration. This finding is in contradiction to that of Clark and Graybiel (Ref. 5) who reported a higher threshold value for deceleration than acceleration. In a pilot study conducted to establish acceleration/deceleration levels for Experiment 1, these were initially established to bracket the values of .02 g for the acceleration threshold and .08 g for the deceleration threshold as reported by Clark and Graybiel (Ref. 5). Subjects were able to detect decelerations with near-perfect accuracy. This led to use of orthogonal combination of absolute $\Delta V/\Delta T$ values and ΔV sign for the main study with the resulting small but statistically significant increment in deceleration as compared with acceleration.

The remaining significant sources of variance in Table 3-2 deal with $\Delta V/\Delta T$, ΔT cases studied. To provide a means for generalizing the data obtained, it was considered necessary to provide a regression equation for correct detection probability as a function of absolute acceleration level and duration of the acceleration. The development of a functional form follows Guedry (Ref. 14) in supposing that the vestibular system response should be proportional to acceleration with an exponential lag for modest acceleration values. A simple equation for a "detectability figure of merit" would then be:

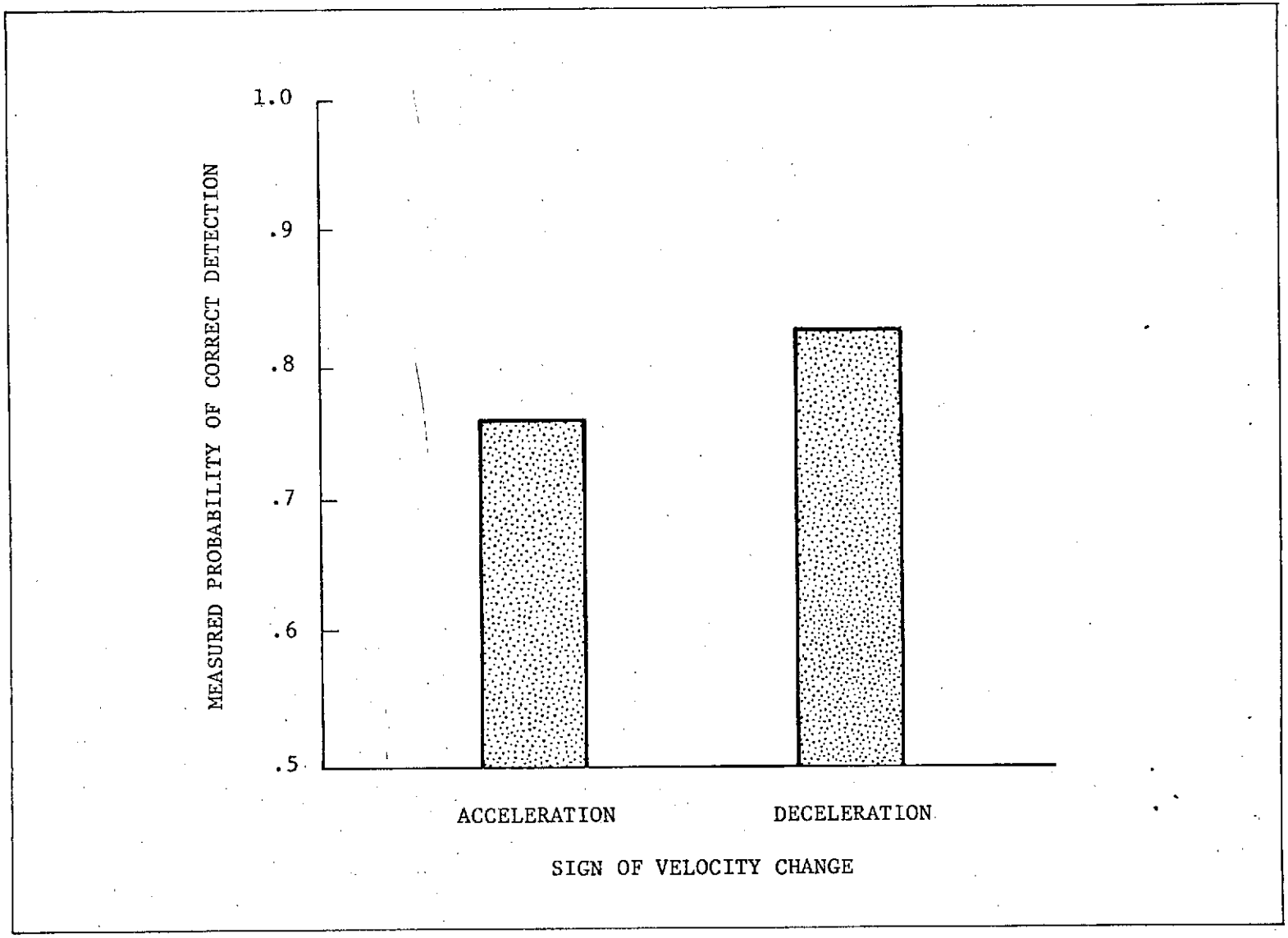

FIGURE 3-2. Measured Probability of Correct Detection of X-Axis Velocity Change as a Function of Sign of Velocity Change

$$D_x = a(1 - e^{-T}) \qquad (3\text{-}1)$$

Where D_x = figure of merit

a = absolute value of $\Delta V/\Delta T$ (ft/sec^2)

T = ΔT (sec)

Eq. (3-1) does not need to be an exact model of vestibular dynamics but it does accord with theories of vestibular functioning. Table 3-3 gives the calculated values of D_x for the acceleration and duration levels employed here.

If D_x serves as a figure of merit for detectability, detection probability should be related to D_x in the following ways:

- Detection probability (P) should increase monotonically with D_x.
- The limit of P as D_x approaches infinity should be 1.00.
- P should equal .50 when $D_x = 0$.

A simple functional relationship which meets these requirements is:

$$P = 1 - .50e^{-bD_x} \qquad (3\text{-}2)$$

Eq. (3-2) was employed as a functional form for fitting a regression line to the data. To reflect the significant interaction effects found in Table 3-2, the free parameter b was estimated separately for the four combinations of sign of velocity change and direction of travel. This analysis was performed using smoothed probability data based on the analysis of variance model with terms dropped based on the results of the analysis of variance F tests.

To estimate b, it is necessary to take logarithms on both sides of eq. (3-2):

$$\log \frac{1 - P}{.50} = -bD_x \log e \qquad (3\text{-}3)$$

TABLE 3-3

DETECTABILITY FIGURE OF MERIT
FOR EXPERIMENT 1

Case	$a(ft/sec^2)$	a(g)	ΔT	D_x
1	.193	.006	.5	.076
2	.386	.012	.5	.152
3	.611	.019	.5	.240
4	.997	.031	.5	.392
5	1.512	.047	.5	.595
6	.611	.019	1.0	.386
7	.997	.031	1.0	.630
8	.193	.006	1.5	.150
9	.386	.012	1.5	.300
10	.611	.019	1.5	.475

Assuming natural logarithms are used:

$$\log e \frac{1 - P}{.50} = bD_x \tag{3-4}$$

Eq. (3-4) has the general form of a linear function with zero intercept:

$$A = bD_x \qquad \text{Where } A = \log e \frac{1 - P}{.50} \tag{3-5}$$

To estimate b, the error of estimation is:

$$E = A - bD_x \tag{3-6}$$

And the sum of squared errors is:

$$\Sigma E^2 = \Sigma A^2 - 2b\Sigma AD_x + b^2\Sigma D_x^2 \tag{3-7}$$

Least squares estimation then requires the first derivative of eq. (3-7) with respect to the parameter:

$$\frac{d\Sigma E^2}{db} = -2\Sigma AD_x + 2b\Sigma D_x^2 \tag{3-8}$$

Setting eq. (3-8) to zero:

$$\Sigma AD_x = b\Sigma D_x^2 \tag{3-9}$$

and

$$\tilde{b} = \frac{\Sigma AD_x}{\Sigma D_x} \tag{3-10}$$

A difficulty arises at this point since estimation of $\underline{b}$ by means of eq. (3-10) does not necessarily reduce the sum of errors to zero. Fitting a non-zero intercept would satisfy both estimation properties but would result in P taking on some value other than .50 when $D_x = 0$. The $\underline{b}$ estimate which does reduce the sum of errors to zero may be obtained by summing of eq. (3-6):

$$\Sigma E = \Sigma A - b\Sigma D_x \tag{3-11}$$

Setting eq. (3-6) to zero:

$$\hat{b} = \frac{\Sigma A}{\Sigma D_x} = \frac{\overline{A}}{\overline{D}_x} \tag{3-12}$$

Estimation was carried out separately using eqs. (3-10) and (3-12) and since the results were found to agree within a few percent, the presented $\underline{b}$ values are based on eq. (3-12). These estimates are shown in Table 3-4. The data points and fitted functions are shown in Figures 3-3 to 3-6. The function values for a particular level of D_x should be used to determine the detection accuracy for interpolated values of $\frac{\Delta V}{\Delta T}$ and ΔT. The curves for the four combinations of levels of motion direction and sign of velocity change represent smoothed data which reflect the main trends isolated by the analysis of variance.

TABLE 3-4

ESTIMATES OF THE DETECTABILITY PARAMETER b
FOR X-AXIS VELOCITY CHANGE

Motion Direction	Velocity Change	$\tilde{b}$
Forward	Acceleration	-1.960
Aft	Acceleration	-2.458
Forward	Deceleration	-3.137
Aft	Deceleration	-3.695

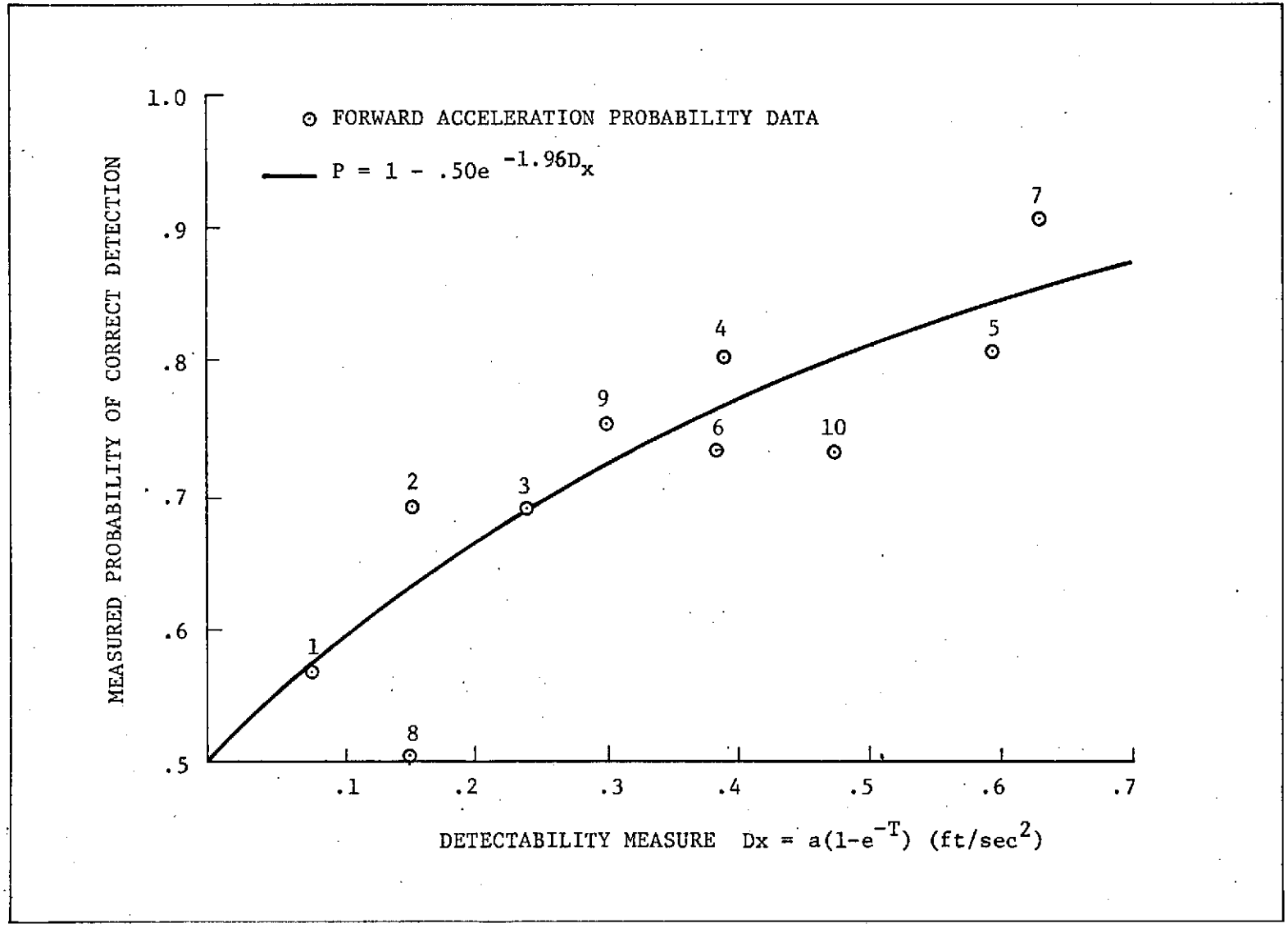

FIGURE 3-3. Measured Probability of Correct Detection of X-Axis Forward Acceleration as a Function of Absolute Value of Acceleration and Interval Duration. Numbers in Graph Refer to Cases 1-10.

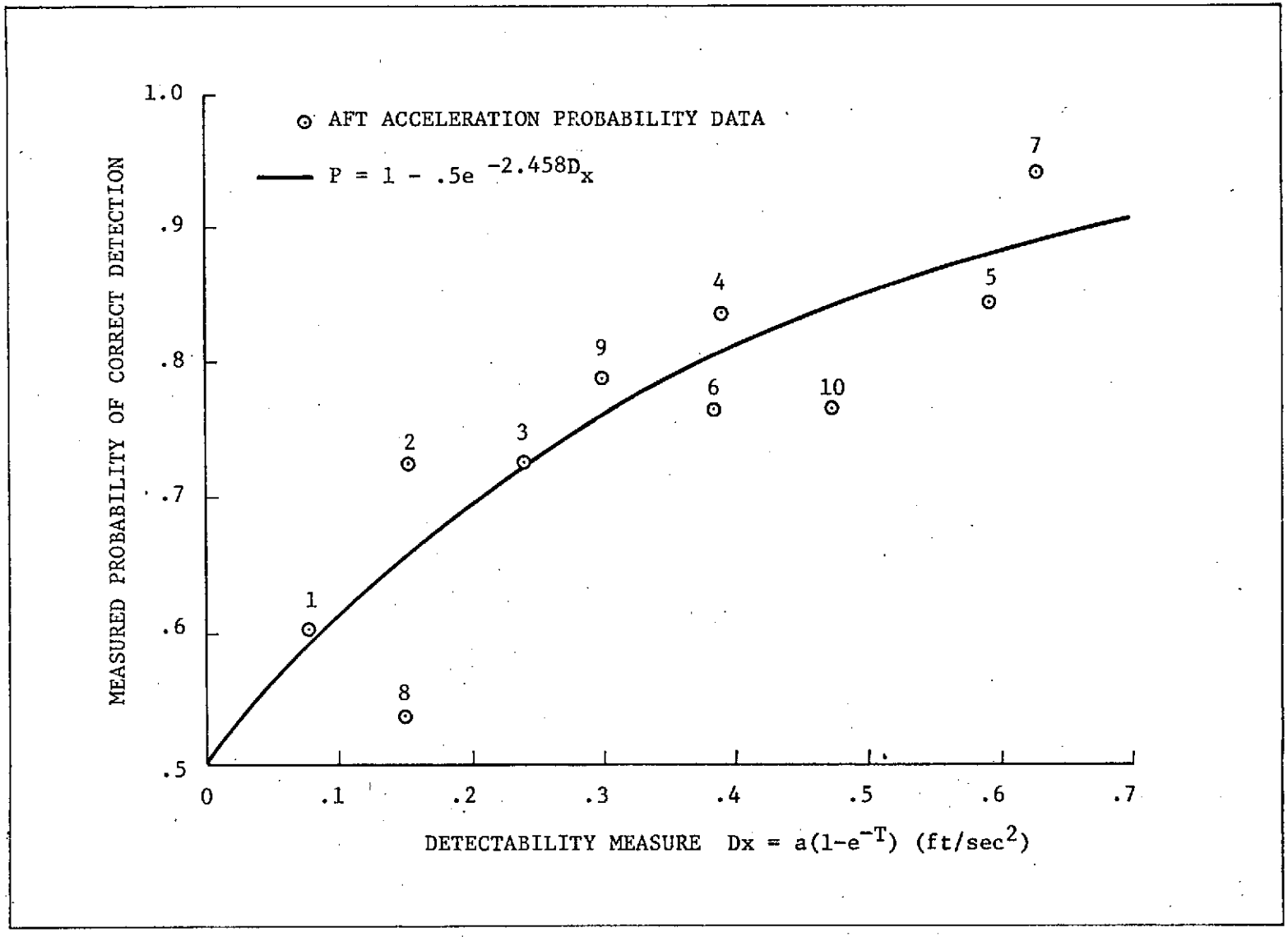

FIGURE 3-4. Measured Probability of Correct Detection of X-Axis Aft Acceleration as a Function of Absolute Value of Acceleration and Interval Duration. Numbers in Graph Refer to Cases 1-10.

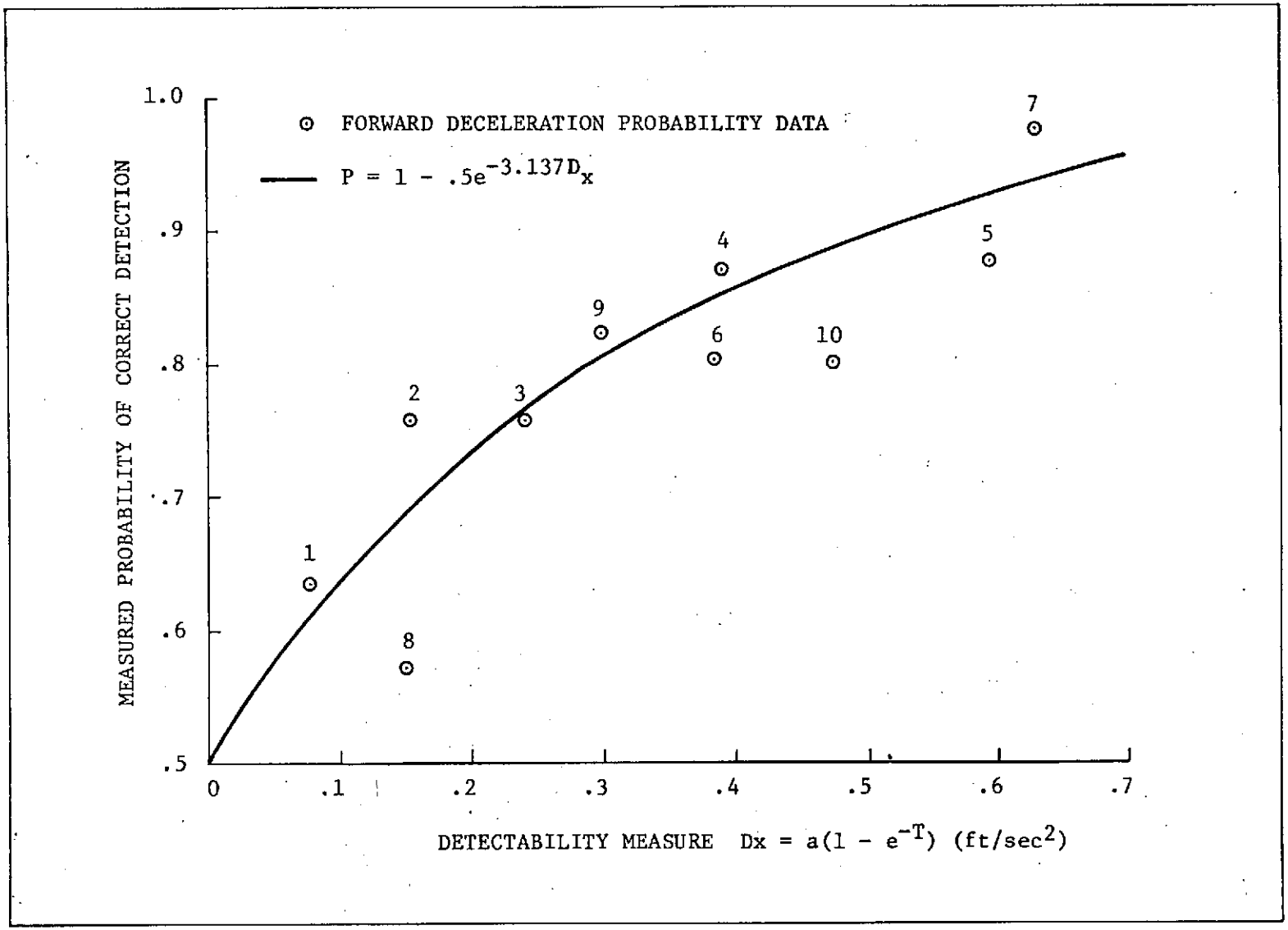

FIGURE 3-5. Measured Probability of Correct Detection of X-Axis Forward Deceleration as a Function of Absolute Value of Deceleration and Interval Duration. Numbers in Graph Refer to Cases 1-10.

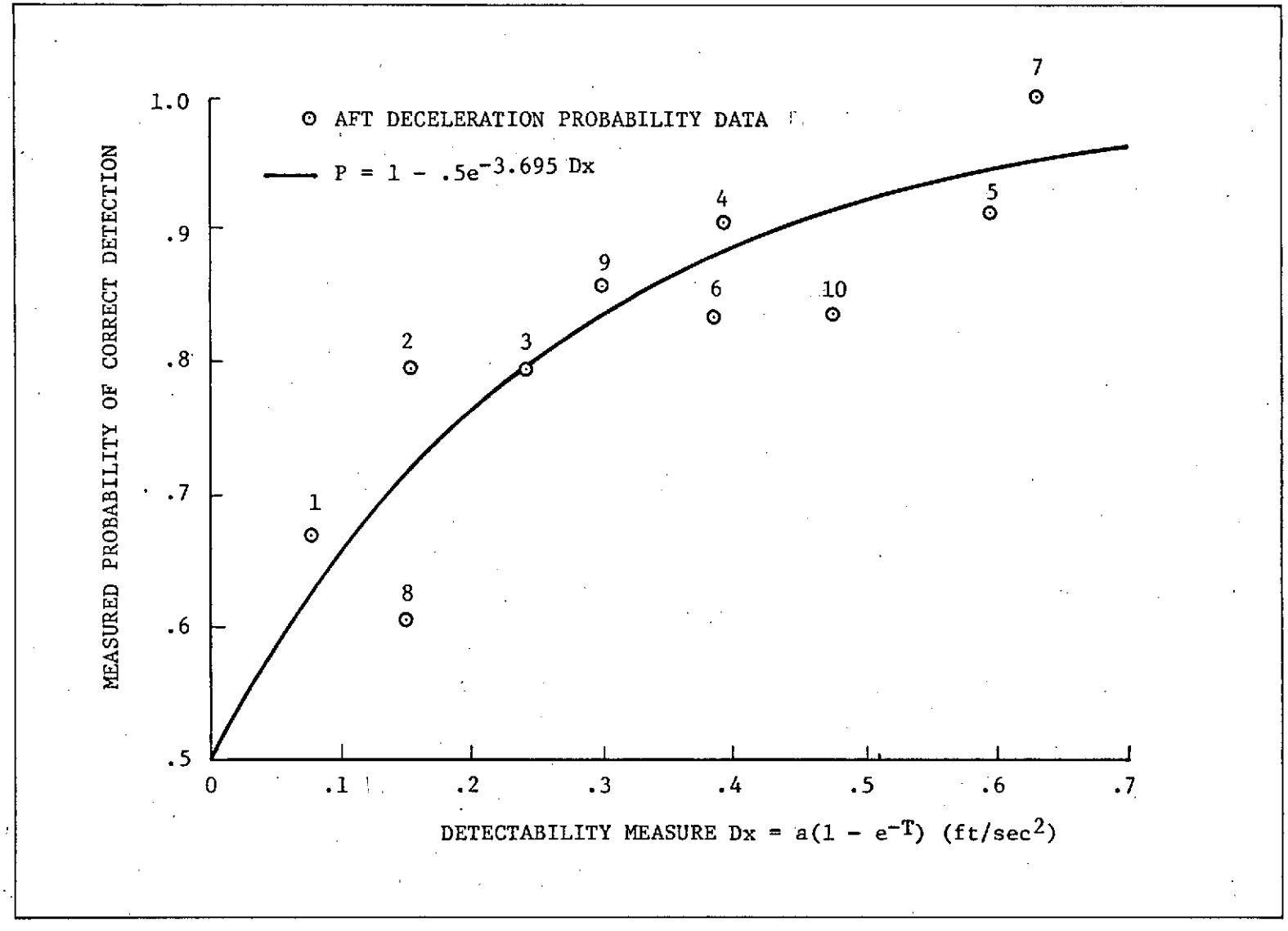

FIGURE 3-6. Measured Probability of Correct Detection of X-Axis Aft Deceleration as a Function of Absolute Value of Deceleration and Interval Duration. Numbers in Graph Refer to Cases 1-10.

4.0 EXPERIMENT 2 - VERTICAL MOTION SIGNAL DETECTION

4.1 - Objective

The objective of Experiment 2 was to measure linear acceleration sensitivity in the vertical (± Z) axis. Data were collected under baseline conditions and then with contradictory cues introduced.

4.2 - Apparatus

The apparatus consisted of the same equipment described in Experiment 1.

4.3 - Experimental Design

Five independent variables were manipulated in Experiment 2. These variables and their levels were as follows:

Test Condition	Baseline (no visual cues) or contradictory (steering plus visual scene constant forward velocity)
Direction of Motion	Up or Down
Velocity Change	Acceleration or Deceleration
Test Signal Duration	0.5 or 1.0 seconds
Magnitude of Velocity Change	0.097 to 1.191 ft/sec^2 (0.003 to 0.037g)

The levels of test signal duration and velocity change magnitude are shown in Table 4-1.

Seven subjects performed the tests at all possible combinations of levels of the independent variables. Each subject completed a block of 40 trials under one of the two test conditions before going to the next block of 40 trials. The order of presentation of specific treatment levels was randomized per block of 40 trials.

TABLE 4-1

ABSOLUTE MAGNITUDE OF VELOCITY CHANGE AND INTERVAL DURATION FOR EXPERIMENT 2

Case	ΔT	g	ft/sec^2	cm/sec^2
1	.5	.003	.097	2.957
2	.5	.005	.161	4.907
3	.5	.009	.291	8.871
4	.5	.012	.386	12.429
5	.5	.025	.805	25.921
6	.5	.037	1.191	36.314
7	1.0	.005	.161	4.907
8	1.0	.009	.291	8.871
9	1.0	.025	.805	25.921
10	1.0	.037	1.191	36.314

The dependent measure employed was detection response accuracy.

4.4 - Procedure

The procedure was identical to that for Experiment 1 for baseline and for contradictory cues.

4.5 - Results and Data Analyses

Signal detection accuracy was scored as being correct or incorrect based upon test interval selected versus interval signal presented.

These data were subjected to a five-way analysis of variance assuming a treatments by subject design and all factors except subjects fixed. The resulting analysis of variance table for signal detection accuracy is presented in Table 4-2.

The significant sources of variance identified in Table 4-2 were the case main effect and the interaction of motion direction, sign of velocity change, and case. Therefore, the same analysis discussed in connection with Experiment 1 was carried out. In the case of vertical motion, the detectability figure of merit is denoted D_z. Table 4-3 gives values of D_z for the combinations of velocity change and interval duration studied. Case effects were fitted separately for the four combinations of motion direction and direction of velocity change. The parameter b has the same interpretation as in connection with Experiment 1. The estimates of b coefficients are shown in Table 4-4. The corresponding functions and data points are depicted in Figures 4-1 through 4-3.

ANALYSIS OF VARIANCE OF Z-AXIS
VELOCITY CHANGE DETECTION PROBABILITY

Source	df	SS	MS	F
Test Condition (T)	1	.03	.03	.21
Direction of Travel (D)	1	.03	.03	.15
$\pm \Delta V$ (G)	1	.18	.18	.18
Case (C)	9	10.32	1.15	4.42**
Subjects (S)	6	3.51	.58	--
T x D	1	.03	.03	.08
T x G	1	.06	.06	.27
T x C	9	2.15	.24	1.39
T x S	6	.81	.13	--
D x G	1	.86	.86	2.79
D x C	9	1.44	.16	.66
D x S	6	1.15	.19	--
G x C	9	4.00	.44	1.77
G x S	6	6.01	1.01	--
C x S	54	14.00	.26	--
T x D x G	1	.18	.18	.93
T x D x C	9	1.29	.14	.75
T x D x S	6	2.15	.36	--
T x G x C	9	1.26	.14	.84
T x G x S	6	1.41	.23	--
T x C x S	54	9.27	.17	--
D x G x C	9	3.60	.40	2.18*
D x G x S	6	1.86	.31	--
D x C x S	54	13.14	.24	--
G x C x S	54	13.57	.25	--
T x D x G x C	9	1.86	.21	1.23
T x D x C x S	54	10.28	.19	--
T x G x C x S	54	9.02	.17	--
T x G x C x S	54	9.92	.18	--
T x D x G x C x S	54	9.07	.17	--
TOTAL	559	133.57		

* Significant at the .05 level
** Significant at the .01 level

TABLE 4-3

DETECTABILITY FIGURE OF MERIT
FOR EXPERIMENT 2

Absolute Velocity Change

Case	ΔT	g	ft/sec^2	cm/sec^2	D_z
1	.5	.003	.097	2.975	.038
2	.5	.005	.161	4.907	.063
3	.5	.009	.291	8.871	.114
4	.5	.012	.386	12.429	.152
5	.5	.025	.805	25.921	.317
6	.5	.037	1.191	36.314	.469
7	1.0	.005	.161	4.907	.102
8	1.0	.009	.291	8.871	.184
9	1.0	.025	.805	25.921	.509
10	1.0	.037	1.191	36.314	.753

TABLE 4-4

ESTIMATES OF THE DETECTABILITY PARAMETER b
FOR Z-AXIS VELOCITY CHANGE

Motion Direction	Velocity Change	$\hat{b}$
Up	Acceleration	-1.201
Down	Acceleration	-0.606
Up	Deceleration	-1.201
Down	Deceleration	-2.205

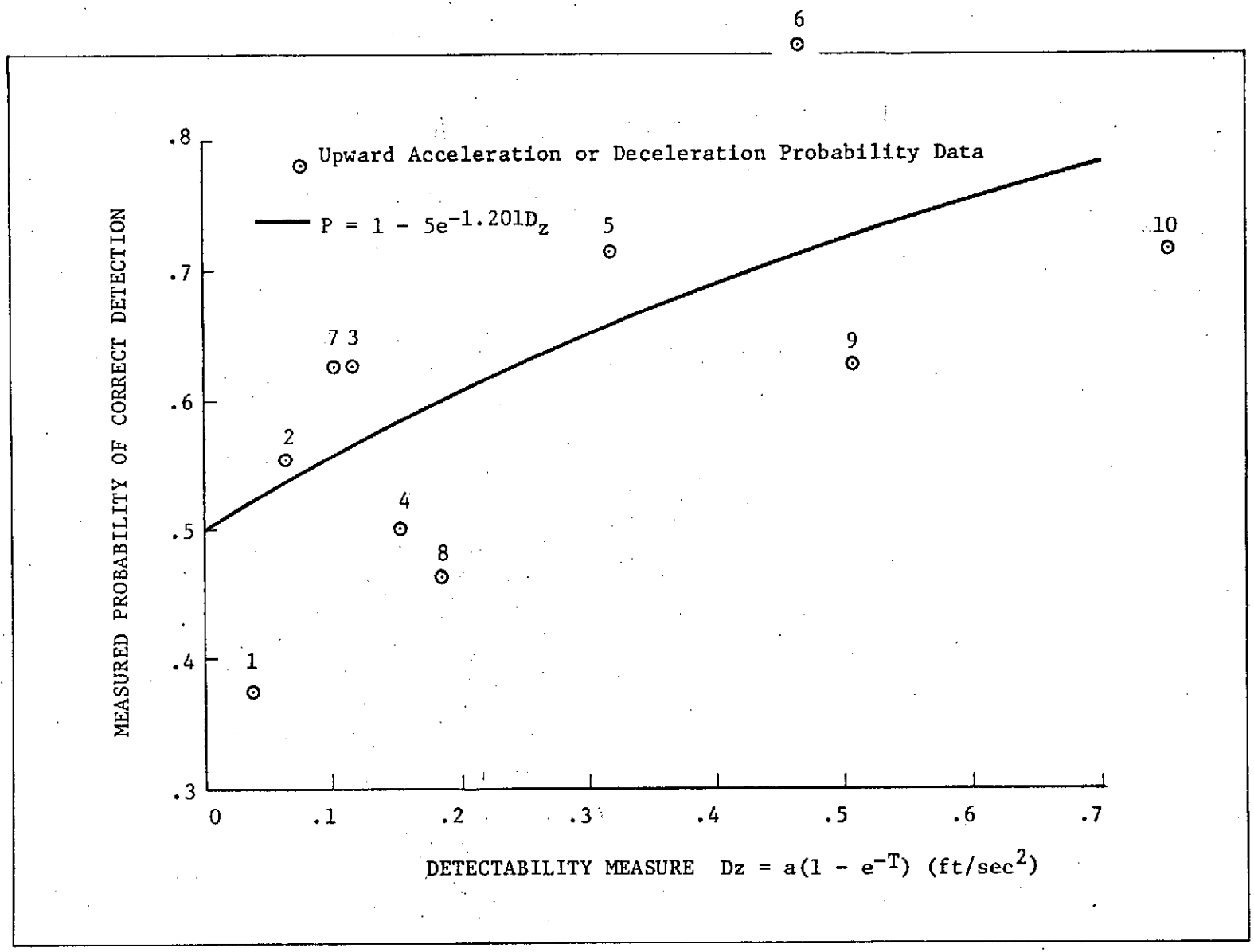

FIGURE 4-1. Measured Probability of Correct Detection of Z-Axis Upward Acceleration or Deceleration as a Function of Absolute Value of Acceleration or Deceleration and Interval Duration. Numbers in Graph Refer to Cases 1-10.

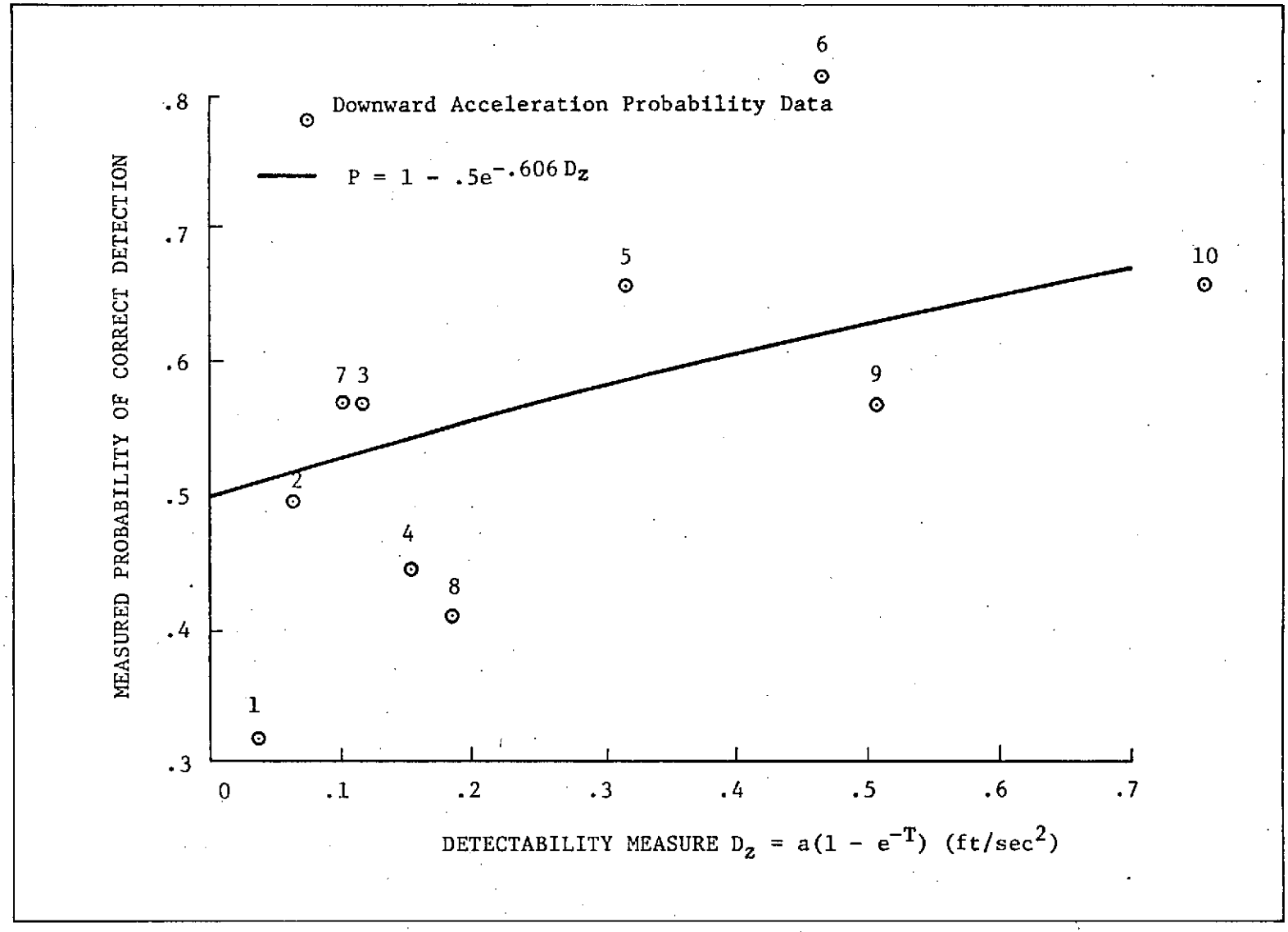

FIGURE 4-2. Measured Probability of Correct Detection of Z-Axis Downward Acceleration as a Function of Absolute Value of Acceleration and Interval Duration. Numbers in Graph Refer to Cases 1-10.

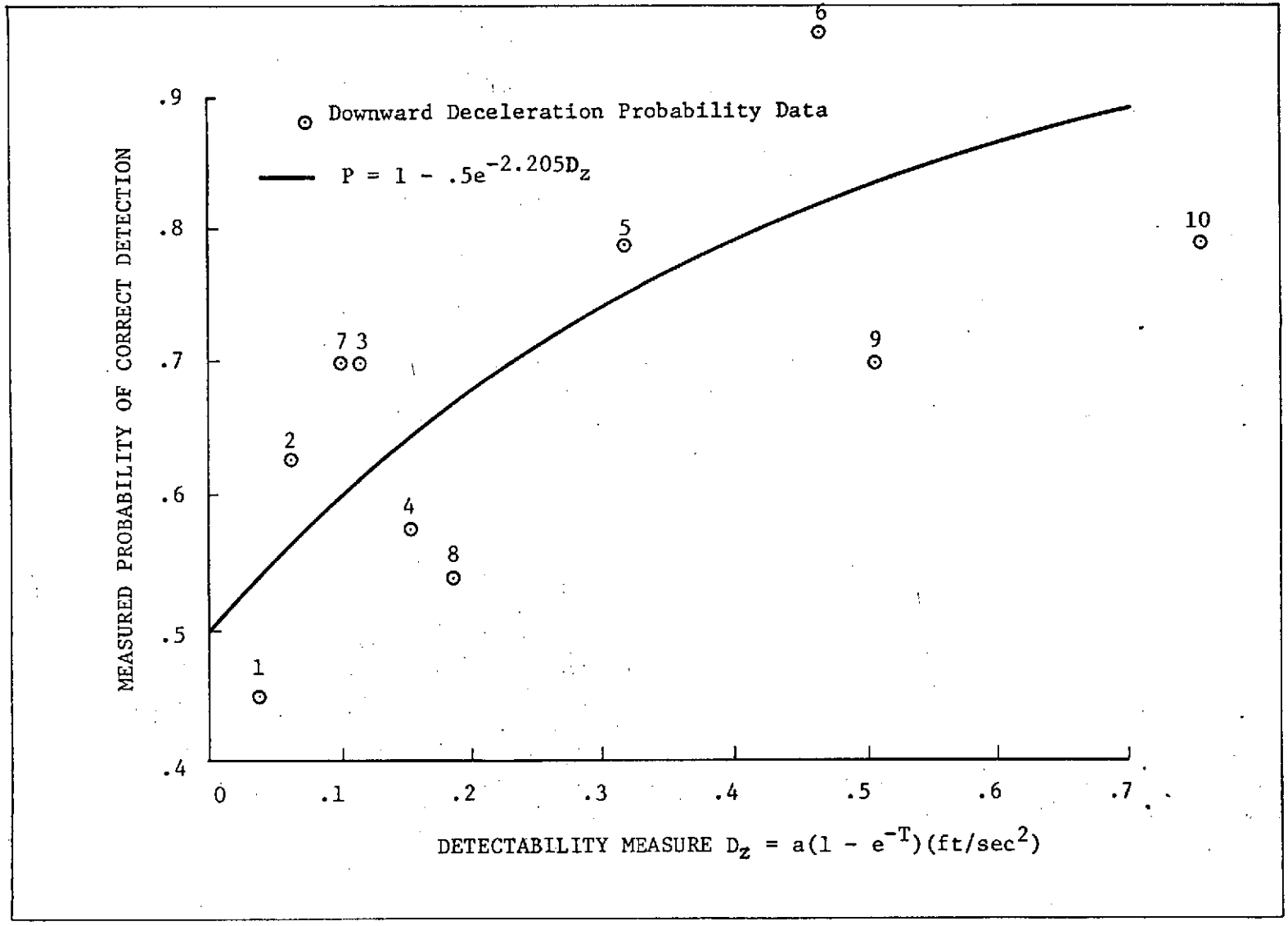

FIGURE 4-3. Measured Probability of Correct Detection of Z-Axis Downward Deceleration as a Function of Absolute Value of Deceleration and Interval Duration. Numbers in Graph Refer to Cases 1-10.

5.0 EXPERIMENT 3 - PITCH MOTION SIGNAL DETECTION

5.1 - Objective

The objective of Experiment 3 was to measure angular acceleration sensitivity in the pitch up - pitch down directions. Data were collected under baseline conditions and then when contradictory cues were introduced.

5.2 - Apparatus

The apparatus was the same as that used in Experiment 1.

5.3 - Experimental Design

Five independent variables were manipulated in Experiment 3. These variables and their levels were as follows:

Test Condition	Baseline (no visual cues) or contradictory (steering plus visual scene with constant forward velocity)
Direction of Motion	Pitch Up or Pitch Down
Velocity Change	Acceleration or Deceleration
Test Signal Duration	0.75 or 1.25 seconds
Magnitude of Velocity Change	1 to 5 degrees/sec^2

The combinations of signal duration and magnitude of velocity change employed are shown in Table 5-1.

Ten subjects performed the tests at all possible combinations of levels of the independent variables. Each subject completed a block of 40 trials under one of the two test conditions before going to the next block of 40 trials. The order of presentation of specific treatment levels was randomized per block of 40 trials.

5.4 - Procedure

The procedure was the same as previous experiments. The subjects were allowed practice steering along the road with no base motion prior to actual testing. During the testing their only criterion for steering was that they attempt to stay within the confines of the road.

5.5 - Results and Data Analyses

Signal detection was scored as being correct or incorrect based upon test interval selected versus interval the signal was presented.

These data were subjected to a five-way analysis of variance assuming treatments by subjects design and all factors except subjects fixed. The resulting analysis of variance table for signal detection accuracy is presented in Table 5-2.

Table 5-2 shows that test condition, travel direction, and velocity change direction interact with case although no variable other than case was found to exert a significant main effect. Consequently, curves were fitted to the case effects separately for each combination of travel direction and direction of velocity change. Only the data from the steering task condition were employed since introduction of the task was found to reduce acceleration sensitivity under the acceleration conditon.

The figure of merit employed for pitch acceleration sensitivity is exactly analogous to that for translation and is presented in Table 5-1. Angular acceleration was substituted for linear acceleration so that:

$$D_\theta = \alpha(1 - e^{-T}) \qquad (5\text{-}1)$$

Where:

D_θ = angular acceleration figure of merit
α = absolute change in angular velocity - degrees/sec^2
T = interval duration - sec

TABLE 5-1

ABSOLUTE MAGNITUDE OF VELOCITY CHANGE
FOR EXPERIMENT 3

Case	ΔT	Acceleration deg/sec^2	Figure of Merit D_θ
1	.75	1	.528
2	.75	2	1.055
3	.75	3	1.583
4	.75	4	2.110
5	.75	5	2.638
6	1.25	1	.713
7	1.25	2	1.427
8	1.25	3	2.140
9	1.25	4	2.854
10	1.25	5	3.567

TABLE 5-2

ANALYSIS OF VARIANCE OF PITCH-AXIS
VELOCITY CHANGE DETECTION PROBABILITY

Source	df	SS	MS	F
Test Condition(T)	1	.10	.10	.21
Direction of Travel (D)	1	.00	.00	.01
$\pm \Delta V$ (G)	1	.55	.55	1.33
Case (C)	9	6.45	.72	3.45**
Subjects (S)	9	14.70	1.63	--
T x D	1	.01	.01	.13
T x G	1	1.36	1.36	3.31
T x C	9	1.96	.22	.39
T x S	9	4.31	.48	--
D x G	1	.28	.28	.93
D x C	9	2.81	.31	1.99*
D x S	9	1.21	.13	--
G x C	9	3.21	.36	1.66
G x S	9	3.71	.41	--
C x S	81	16.81	.21	--
T x D x G	1	.21	.21	4.22
T x D x C	9	1.30	.14	.95
T x D x S	9	.80	.09	--
T x G x C	9	2.60	.29	2.19*
T x G x S	9	3.70	.41	--
T x C x S	81	14.50	.81	--
D x G x C	9	2.73	.30	1.75
D x G x S	9	1.28	.14	--
D x C x S	81	12.85	.16	--
G x C x S	81	17.40	.21	--
T x D x G x C	9	.90	.10	.87
T x D x G x S	9	.45	.05	--
T x D x C x S	81	12.26	.15	--
T x G x C x S	81	14.08	.17	--
T x D x G x C x S	81	9.31	.11	--
TOTAL	799	162.59		

*Significant at the .05 level
**Significant at the .01 level

TABLE 5-3

ESTIMATES OF THE DETECTABILITY PARAMETER b
FOR PITCH AXIS VELOCITY CHANGE

Motion Direction	Velocity Change	$\hat{b}$
Up	Acceleration	-.225
Down	Acceleration	-.360
Up	Deceleration	-.431
Down	Deceleration	-.238

The function:

$$P = 1 - .50e^{-bD_\theta} \qquad (5\text{-}2)$$

was then fitted to the pitch detection probability data. The estimates of $\underline{b}$ obtained are given in Table 5-3. The smoothed data and functions are shown in Figures 5-1 through 5-4.

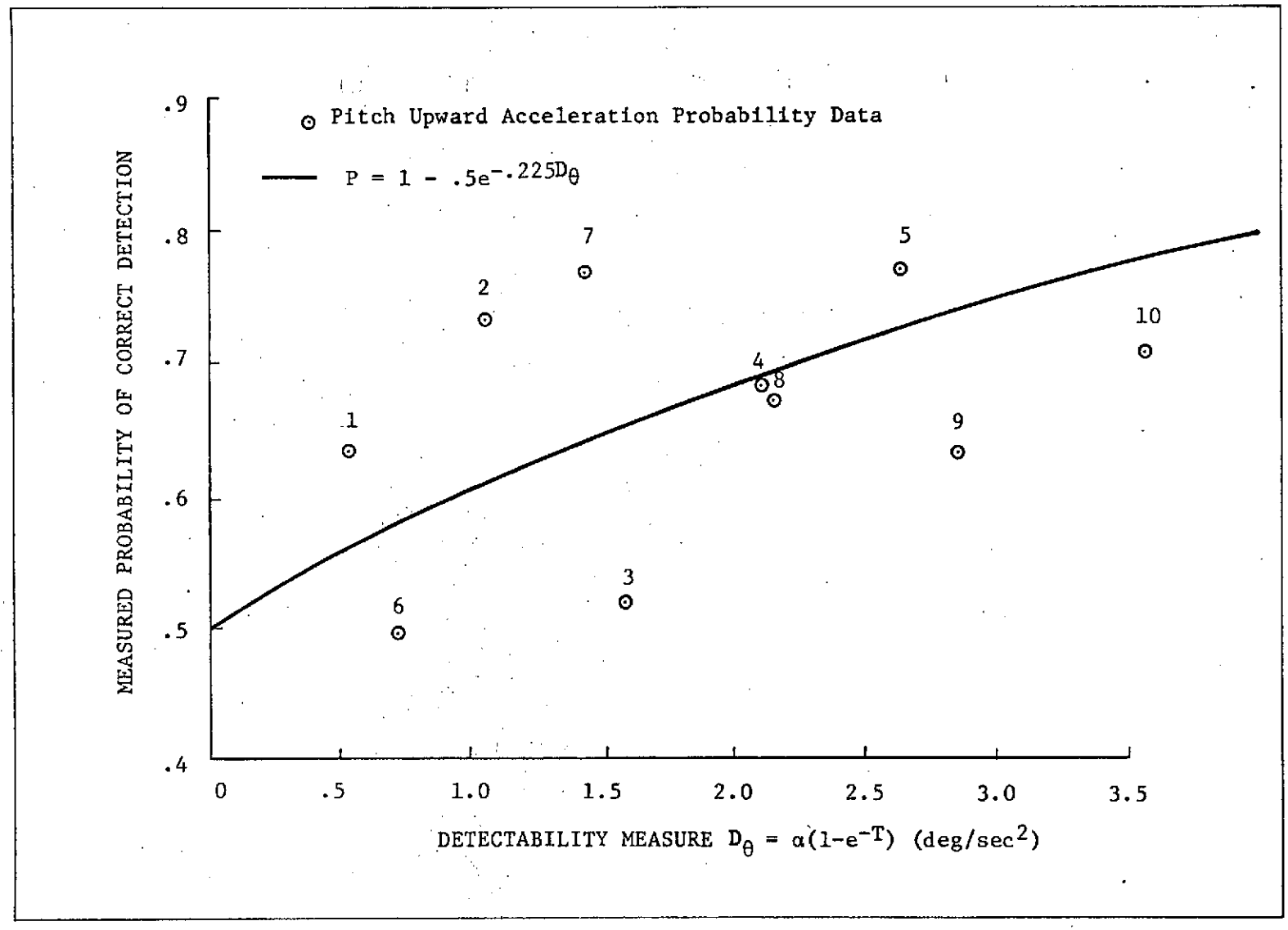

FIGURE 5-1. Measured Probability of Correct Detection of Pitch Axis Upward Angular Acceleration as a Function of Absolute Value of Acceleration and Interval Duration. Numbers in Graph Refer to Cases 1-10.

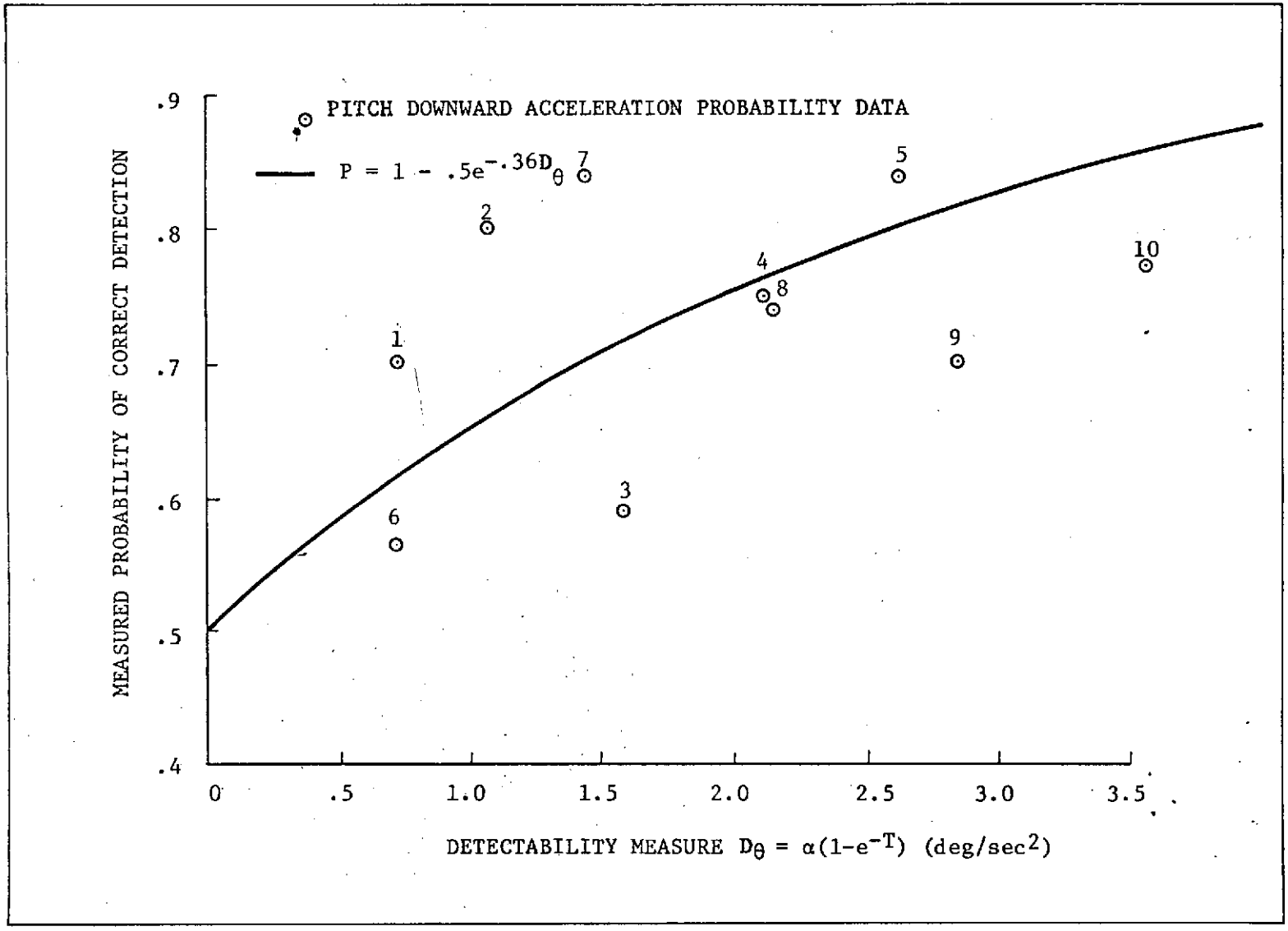

FIGURE 5-2. Measured Probability of Correct Detection of Pitch Axis Downward Angular Acceleration as a Function of Absolute Value of Acceleration and Interval Duration. Numbers in Graph Refer to Cases 1-10.

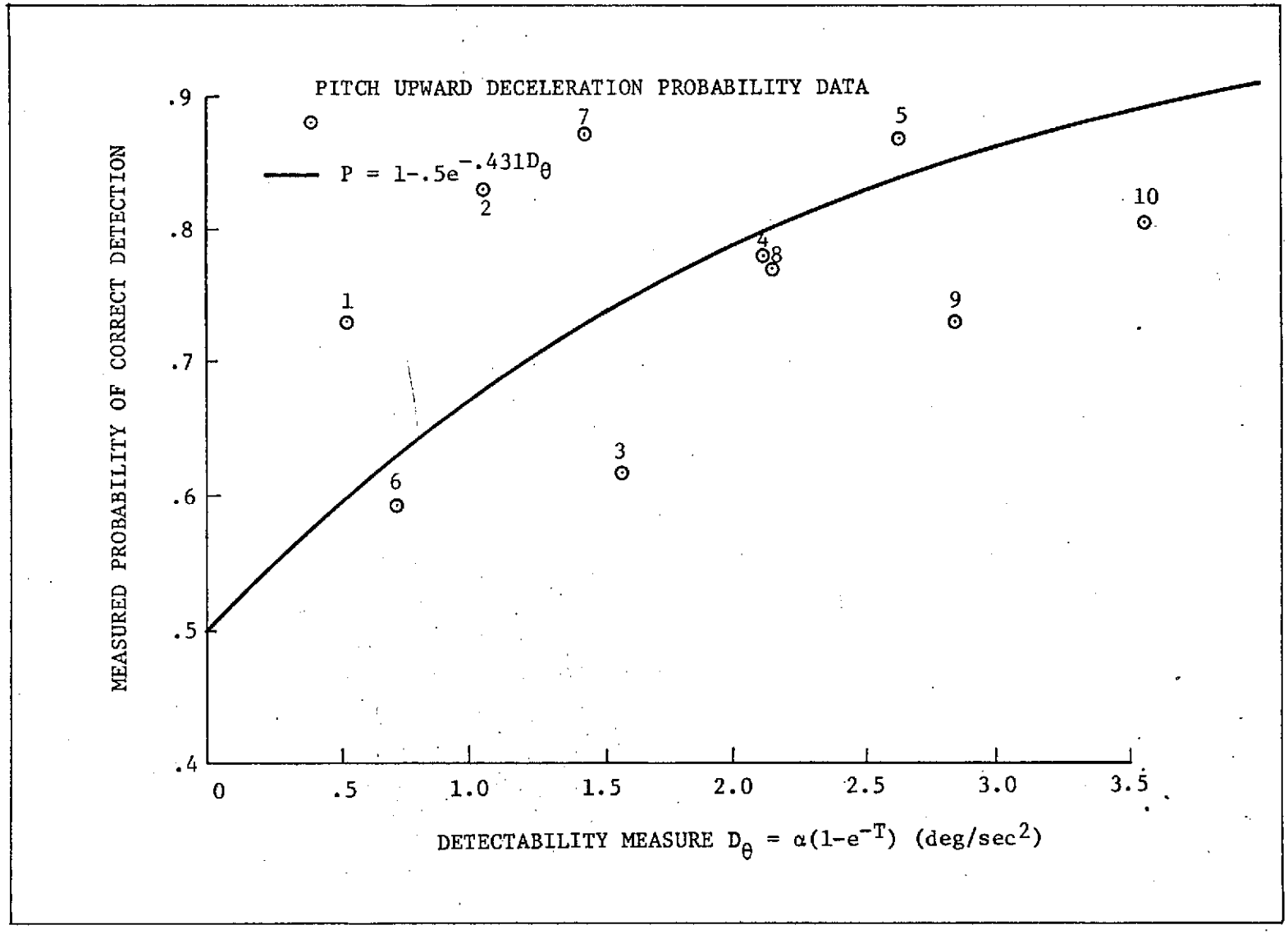

FIGURE 5-3. Measured Probability of Correct Detection of Pitch Axis Upward Angular Deceleration as a Function of Absolute Value of Deceleration and Interval Duration. Numbers in Graph Refer to Cases 1-10.

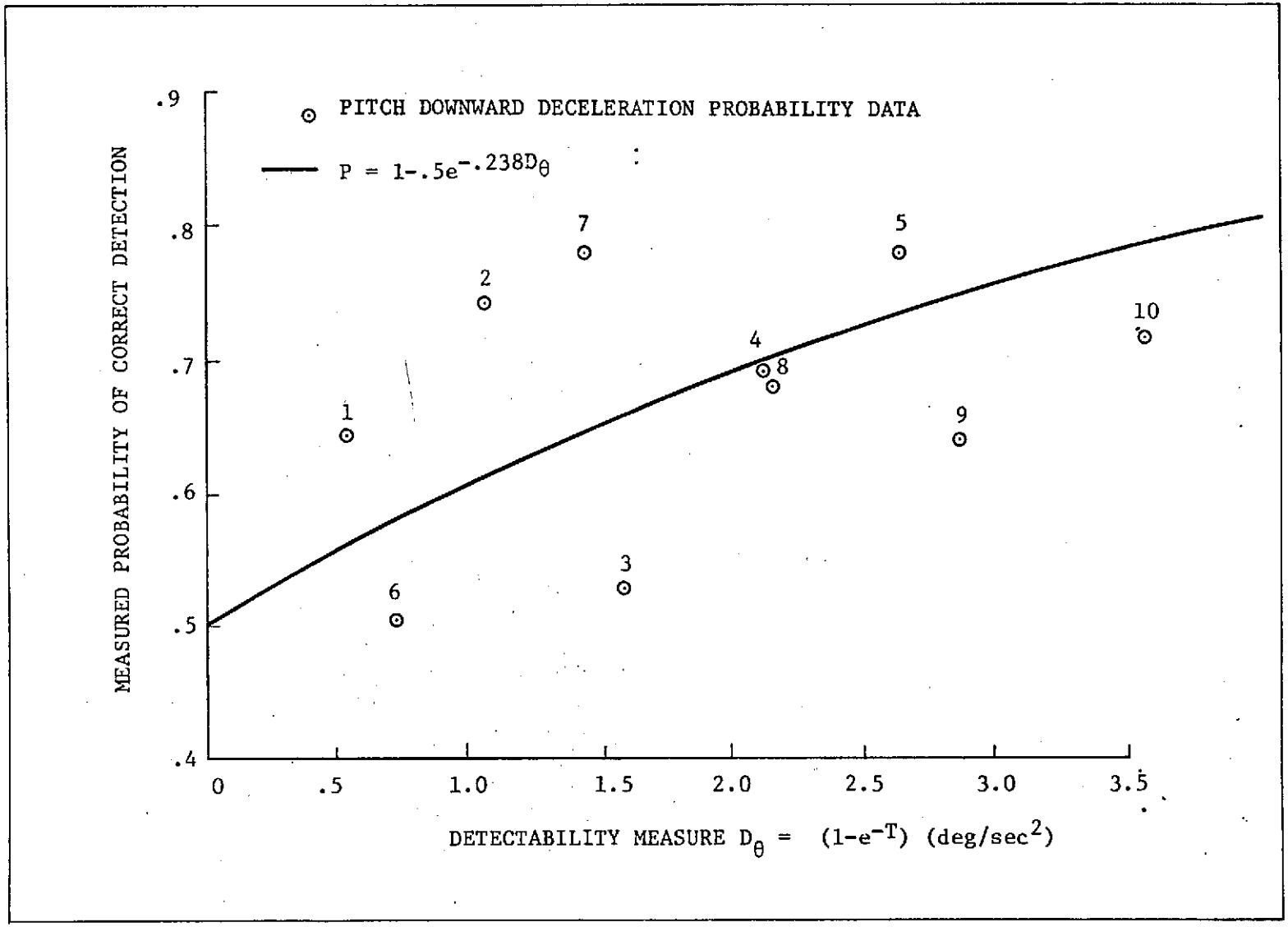

FIGURE 5-4. Measured Probability of Correct Detection of Pitch Axis Downward Angular Deceleration as a Function of Absolute Value of Deceleration and Interval Duration. Numbers in Graph Refer to Cases 1-10.

6.0 DISCUSSION AND RECOMMENDATIONS

6.1 - Summary of Present Data

The functions fitted to the detection probability data from all three experiments are summarized in Table 6-1. Table 6-1 shows the relevant fitted function for each axis, direction of motion, and direction of velocity change. As an example, consider forward acceleration in the X axis. From Table 6-1, the probability of detection data were found to be described by the regression equation:

$$P = 1 - .5e^{-1.96D_x} \qquad (6\text{-}1)$$

Where:

- P = Detection probability for a specific combination of $\Delta V/\Delta T$ and ΔT
- e = Natural log base
- -1.96 = Value of the parameter b fitted to the relevant data from Section 3.0
- D_x = Detectability figure of merit for $\Delta V/\Delta T$ and ΔT combinations for translation in the X axis

D_x is also defined in Table 6-1 as:

$$D_x = a(1 - e^{-T}) \qquad (6\text{-}2)$$

Where:

- a = Absolute value of $\Delta V/\Delta T$, presented during an interval
- T = Interval duration - sec

TABLE 6-1 CORRECT DETECTION PROBABILITY FUNCTIONS

Axis	Motion Direction	Velocity Change Direction	Detection Probability Regression Equation	Detectability Figure Of Merit
X	Forward	Acceleration	$P = 1-.5e^{-1.960D_x}$	$D_x = a(1-e^{-T})$
	Aft	Acceleration	$P = 1-.5e^{-2.458D_x}$	a = Absolute value of velocity change (ft/sec^2)
	Forward	Deceleration	$P = 1-.5e^{-3.137D_x}$	
	Aft	Deceleration	$P = 1-.53^{-3.695D_x}$	T = Interval Duration (sec)
Z	Up	Acceleration	$P = 1-.5e^{-1.201D_z}$	$D_z = a(1-e^{-T})$
	Down	Acceleration	$P = 1-.5e^{-.606D_z}$	a = Absolute value of velocity change (ft/sec^2)
	Up	Deceleration	$P = 1-.5e^{-1.201D_z}$	
	Down	Deceleration	$P = 1-.5e^{-2.205D_z}$	T = Interval Duration (sec)
Pitch	Up	Acceleration	$P = 1-.5e^{-.225D_\theta}$	$D_\theta = \alpha(1-e^{-T})$
	Down	Acceleration	$P = 1-.5e^{-.360D_\theta}$	α = Absolute value of angular velocity change (deg/sec^2)
	Up	Deceleration	$P = 1-.5e^{-.431D_\theta}$	
	Down	Deceleration	$P = 1-.5e^{-.238D_\theta}$	T = Interval Duration (sec)

6.2 - Application to Washout Techniques

The regression equations of Table 6-1 yield the best fitting describing functions for the obtained data. Consequently, these equations should be used to calculate acceleration levels for washout methods. To illustrate the application of the data as summarized in Table 6-1 to washout calculations, consider a simulation in which the operator commands a vehicle acceleration in the forward direction (+X). In response, the motion system should be commanded to accelerate simulating the motion of the actual vehicle. In following the acceleration command, however, the cab will acquire a rate which must be nulled or washed out within the travel constraints. The initial acceleration is a proper motion cue and should be at a value detectable by the operator with high probability. The following deceleration, however, is a spurious cue, if detected by the operator, and should therefore be detectable with low probability. To illustrate the use of equations in Table 6-1 in satisfying these objectives, consider the entire process (valid acceleration cue and washout deceleration) as two pure velocity ramp components. The situation is diagrammed in Figure 6-1.

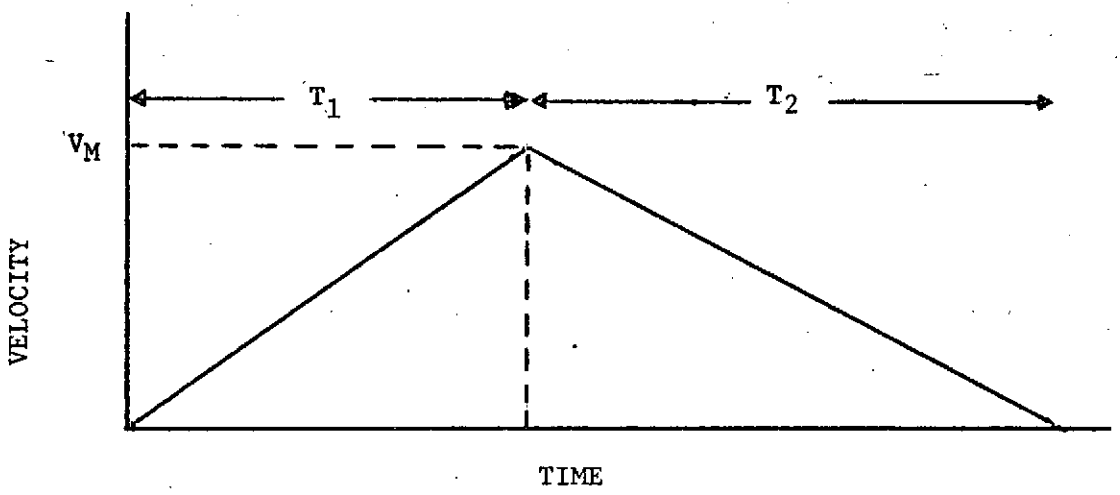

FIGURE 6-1. Velocity Ramp Motion Profile

In Figure 6-1, acceleration takes place during interval 1 and deceleration during interval 2. T_1 and T_2 denote the interval durations and a_1 and a_2 denote the appropriate absolute accelerations. Obviously, the situation shown in Figure 6-1 cannot be obtained in practice since it involves discontinuous motion. The assumption is made here that no smoothing periods are required for acceleration changes to simplify the process of illustrating the general method. If V_M denotes the maximum velocity obtained during the total time interval, then:

$$V_M = a_1T_1 = a_2T_2 \tag{6-3}$$

The average velocity during each time interval is denoted as $\overline{V}$ where:

$$\overline{V} = \frac{V_M}{2} \tag{6-4}$$

Then the total distance travelled during both intervals is:

$$d = \overline{V}(T_1 + T_2) \tag{6-5}$$

These equations may be employed for any of the three axes studied during the present effort. To illustrate the use of the data, three acceleration/washout cases were calculated as shown below:

Axis	Motion Cue	Washout Motion
X	Forward Acceleration	Forward Deceleration
Z	Upward Acceleration	Upward Deceleration
Pitch	Downward Acceleration	Downward Deceleration

To select time interval and acceleration parameters, various constraints may be introduced. One objective is to make the initial acceleration

highly detectable. It will be supposed here that this criterion is satisfied if the acceleration detection probability is equal to .90. The necessary calculations are illustrated below for the case of the X-axis motion sequence.

To introduce the constraint of probability .90 of detecting the initial forward acceleration, the relevant equation from Table 6-1 is:

$$P = 1 - .5e^{-1.96D_x} \tag{6-6}$$

Setting eq. (6-6) to .90 and solving for D_x yields a required value for D_x of .8214. Combinations of a_1 and T_1 which result in $D_x = .8214$ are thus acceptable. D_x is given by the appropriate equation from Table 6-1 as:

$$D_x = a_1(1-e^{-T1}) \tag{6-7}$$

Setting eq. (6-7) equal to .8214 and rearranging yields:

$$a_1 = .8214(1 - e^{-T})^{-1} \tag{6-8}$$

Selecting a value of the initial duration, T_1 then allows calculation of the necessary acceleration to produce a detection probability of .90 via eq. (6-8). For example, if the initial duration is .50 sec.,

$$a_1 = .8214(1 - e^{-.5})^{-1} \tag{6-8}$$

$$a_1 = .8214(1 - .6065)^{-1} \tag{6-9}$$

$$a_1 = .8214(.3935)^{-1} \tag{6-10}$$

$$a_1 = 2.0874 \text{ ft/sec}^2 \tag{6-11}$$

The maximum velocity attained during the motion sequence is then given by eq. (6-3):

$$V_M = a_1T_1 = 2.0874 \text{ ft/sec}^2 \cdot .5 \text{ sec} \tag{6-12}$$

$$V_M = 1.0437 \text{ ft/sec} \tag{6-13}$$

The total distance travelled during the motion sequence is given by eq. (6-5). For the General Purppse Simulator, the constraint on X-axis distance is approximately 8 feet. Setting eq. (6-5) equal to 8 feet.

$$8.0 \text{ ft} = \bar{V} \text{ ft/sec } (T_1 + T_2 \text{ sec}) \tag{6-14}$$

Since:

$$\bar{V} = \frac{V_M}{2} = \frac{1.0437}{2} = .5219 \text{ ft/sec} \tag{6-15}$$

Eq. (6-14) yields a value of $T_1 + T_2$

$$T_1 + T_2 = \frac{8.0 \text{ ft}}{.5219 \text{ ft/sec}} = 15.33 \text{ sec} \tag{6-16}$$

By subtraction, therefore, $T_2 = 15.33 - .50 = 14.83$ sec. The deceleration a_2 necessary to null the maximum velocity is given by:

$$a_2 = \frac{V_M}{T_2} = \frac{1.0437 \text{ ft/sec}}{14.83 \text{ sec}} = .0704 \text{ ft/sec}^2 \tag{6-17}$$

T_2 and a_2 may then be substituted in the X-axis forward deceleration regression equation from Table 6-1 to predict the washout motion detection probability:

$$D_x = a_2(1 - e^{-T2}) = .0704(1 - e^{-14.83}) \tag{6-18}$$

The expression in parentheses is essentially equal to unity for an exponent of -14.83 so that $D_{x2} = .0704$ ft/sec^2. The detection probability is then estimated via the appropriate equation from Table 6-1:

$$P = 1 - .5e^{-3.137D_x} \tag{6-19}$$

$$P = 1 - .5e^{-3.137 \cdot .0704} \tag{6-20}$$

$$P = 1 - .5e^{-.2208} \tag{6-21}$$

$$P = 1 - .5(.8025) \tag{6-22}$$

$$P = .559 \tag{6-23}$$

The above calculations were carried out for a range of interval 1 durations for the three motion sequences listed on page 69 . The results are shown in Figures 6-2 to 6-5.

Figure 6-2 shows the relationships between interval 1 acceleration and duration necessary for a detection probability of .90. The linear acceleration values for X and Z are read from the left-hand ordinate. Angular acceleration is read from the right-hand ordinate. The curves show the relationships:

X-axis	$D_x = .8214$	$= a_1(1 - e^{-T1})$
Z-axis	$D_z = 1.3410$	$= a_1(1 - e^{-T1})$
Pitch-axis	$D_\theta = 4.4720$	$= \alpha_1(1 - e^{-T1})$

which are required for detection probability of .90 in all cases.

Figure 6-3 shows the maximum rate reached as a function of interval 1 duration. Translation velocities for the X and Z axes are shown on the left-hand ordinate. Angular velocity for pitch is shown on the right-hand ordinate. The rate constraints of the General Purpose Simulator are shown as horizontal dashed lines. Figure 6-4 shows total duration and interval 2 durations which result from the travel distance constraints of the General Purpose Simulator and the maximum rate data of Figure 6-3. Figure 6-5 shows the probability of detecting the washout deceleration during interval 2 as a function of total sequence duration.

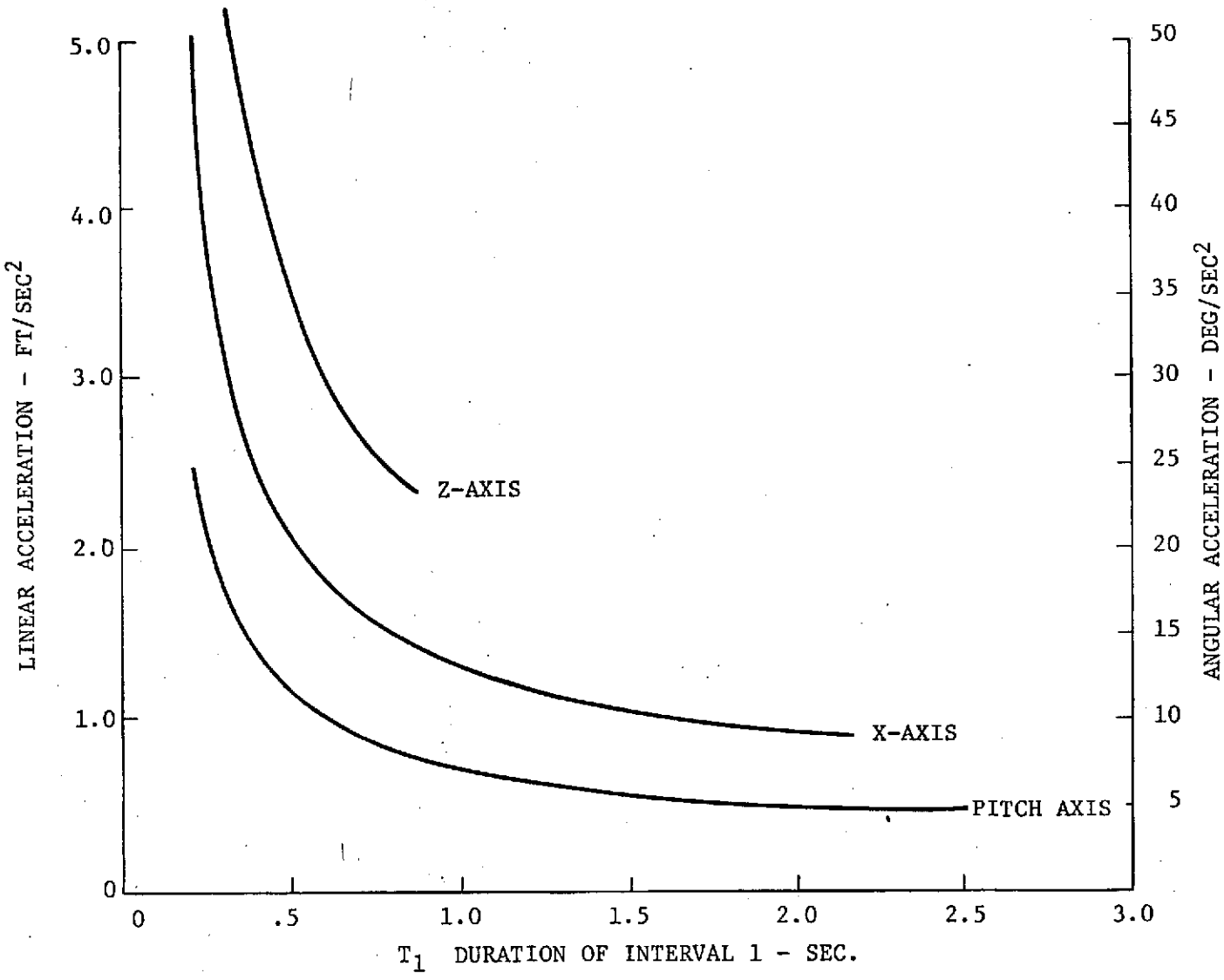

FIGURE 6-2. COMBINATIONS OF ACCELERATION AND INTERVAL 1 DURATION WHICH YIELD A DETECTION PROBABILITY OF .90 FOR THE INITIAL ACCELERATION OF SELECTED MOTION PROFILES

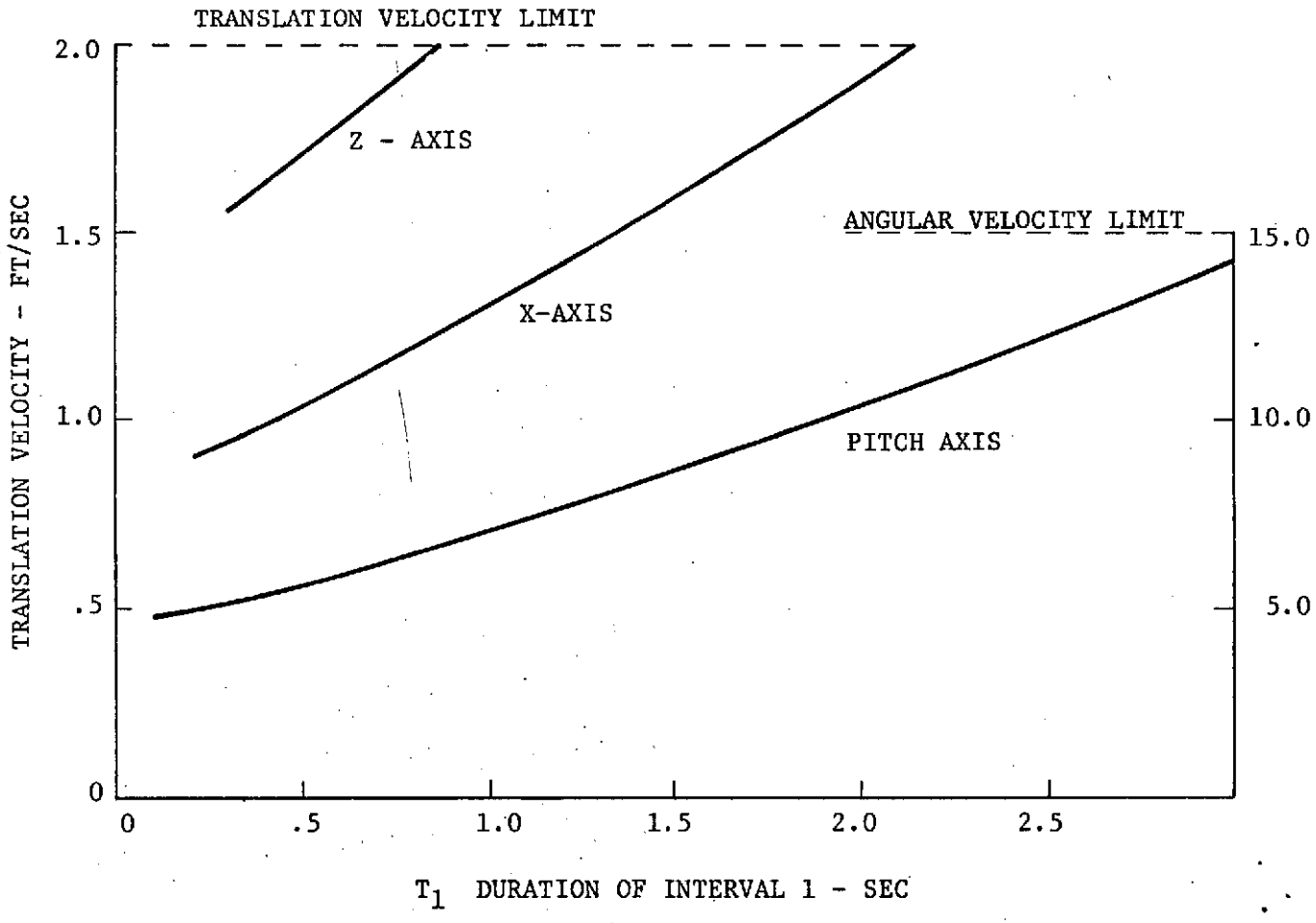

FIGURE 6-3. MAXIMUM VELOCITY REACHED DURING SELECTED MOTION PROFILES

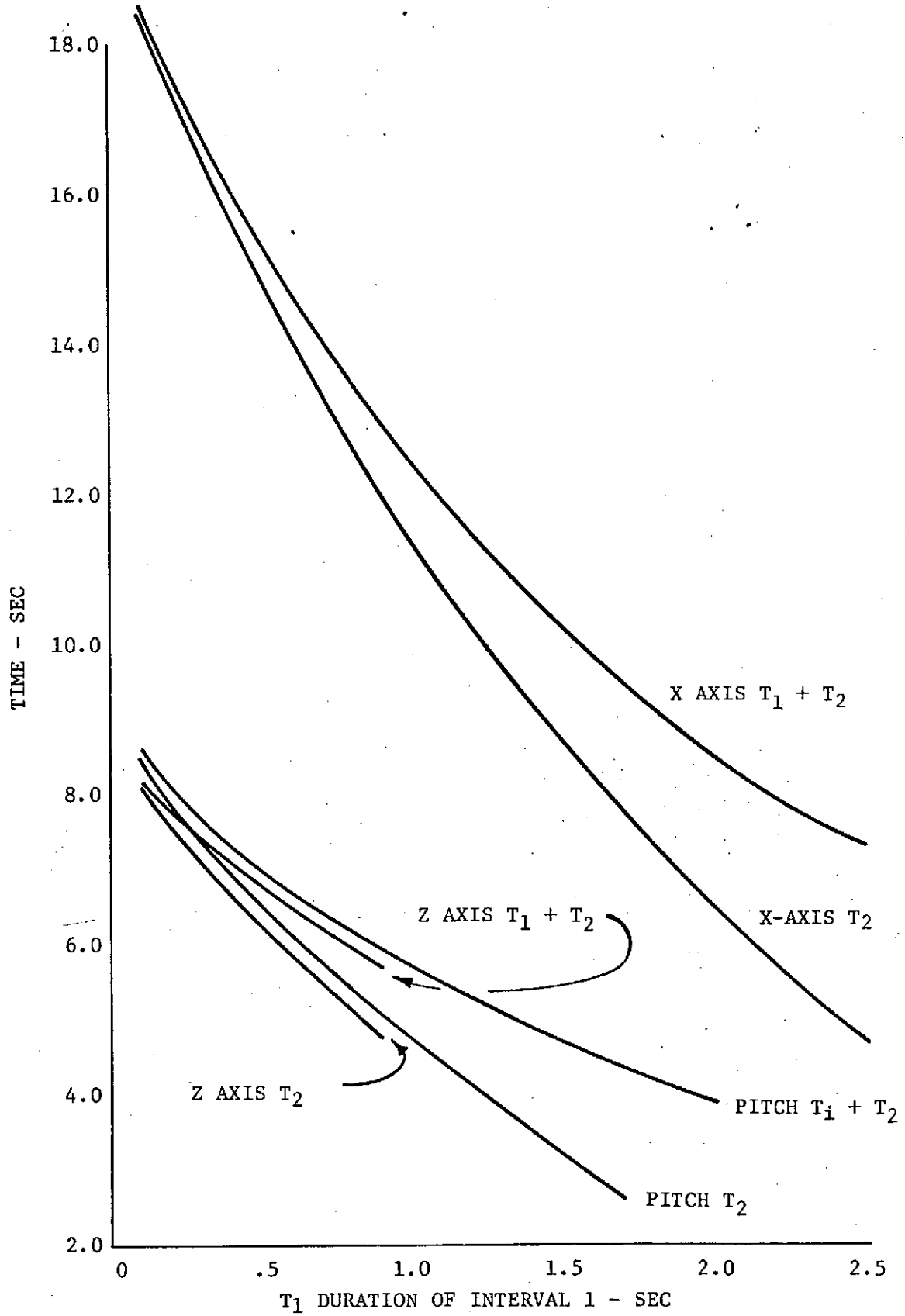

FIGURE 6-4. TOTAL SEQUENCE DURATION AND INTERVAL 2 DURATIONS AS FUNCTIONS OF INTERVAL 1 DURATION FOR SELECTED MOTION PROFILES

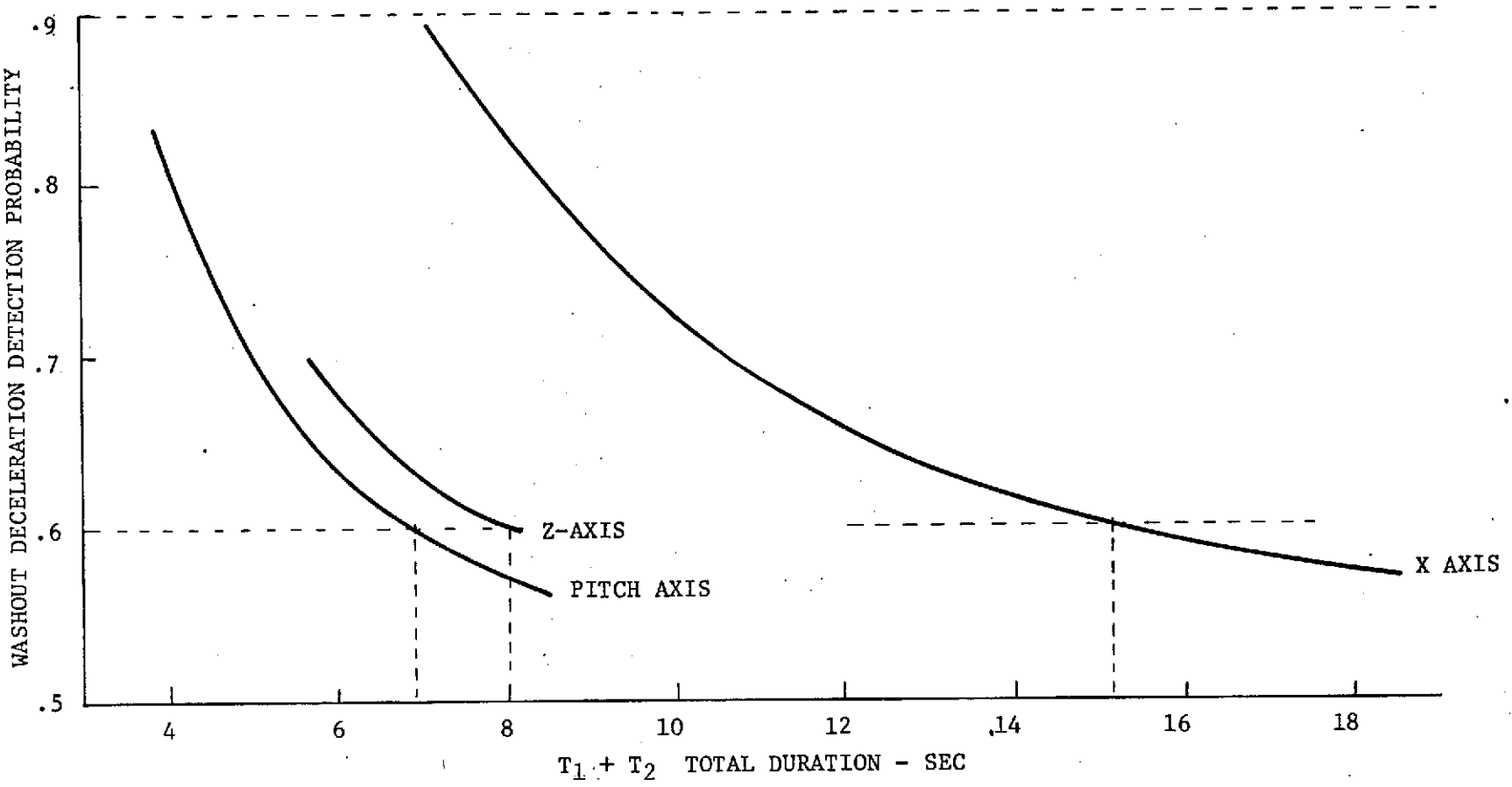

FIGURE 6-5. WASHOUT MOTION DETECTION PROBABILITY AS A FUNCTION OF TOTAL DURATION FOR SELECTED MOTION SEQUENCES

6.3 - Recommended Motion Sequence Parameters

The problem of selecting parameters for the motion sequences is essentially a trade-off based on the data of Figures 6-2 to 6-5. The three axes vary in terms of approaching constraints. Based on these data a set of recommended motion sequence parameters were developed and are shown in Table 6-2. A primary consideration in this analysis was that washout deceleration probability should be kept in the range .60 - .70.

6.3.1 - X-Axis

Selection of interval duration for the X-axis forward acceleration profile does not appear to be strongly constrained by the velocity limit of 2.0 ft/sec. The primary problem is that the data showed subjects to be more sensitive to deceleration than to acceleration as evidenced by the ratio of 1.6 in terms of the b parameters. This produces the requirement for low washout decelerations compared to the initial acceleration and yields large values for the interval 2 duration. Based on Figure 6-5, the X-axis total sequence duration to yield a washout detection probability of .60 is on the order of twice that of the other axes. The primary driving constraint for the X-axis is thus total sequence duration. To reduce this duration to 12 sec, a washout detection probability of .66 was considered acceptable. The motion sequence parameters resulting from this constraint are shown in Table 6-2.

6.3.2 - Z-Axis

In the case of Z-axis upward acceleration, maximum velocity was found to be a limiting factor. The 2 ft/sec velocity constraint of the General Purpose Simulator was found to limit the interval 2 time to about .85 seconds. Reducing the interval 1 duration to about .15 sec would yield a predicted

TABLE 6-2 RECOMMENDED PARAMETERS FOR SELECTED MOTION SEQUENCES

	X-Axis	Z-Axis	Pitch Axis
Motion Cue	Forward Acceleration	Upward Acceleration	Downward Acceleration
Washout Motion	Forward Acceleration	Upward Acceleration	Downward Acceleration
Motion Cue Detection Probability	$.900 = 1-.5e^{-1.96D_{x_1}}$*	$.900 = 1-.5e^{-1.201D_{z_1}}$*	$.900 = 1-.5e^{-.360D_{x_1}}$*
Required Detectability Measure	$D_{x_1} = .8214$ ft/sec^2	$D_{z_1} = 1.341$ ft/sec^2	$D_{\theta_1} = 4.472$ deg/sec^2
Travel Constraint	8.0 ft	5.75 ft	20 deg
Total Time For Motion Sequence	12.000 sec**	6.750 sec	6.300 sec
Interval 1 Duration	1.055 sec	.500 sec**	.750 sec**
Interval 2 Duration	10.945 sec	6.250 sec	5.550 sec
Interval 1 Acceleration	1.264 ft/sec^2	3.408 ft/sec^2	8.476 deg/sec^2
Interval 2 Deceleration	.122 ft/sec^2	.273 ft/sec^2	1.145 deg/sec^2
Maximum Velocity	1.333 ft/sec	1.704 ft/sec**	6.357 deg/sec
Washout Motion Detection Probability	.660**	.640**	.620**

* Input Constraint

** Primary Driver in Parameter Selection

washout detection probability of about .60 with a total duration of about 8.0 seconds. This would involve an interval 1 duration considerably below the value of .5 seconds included in experiment 2 and thus would represent an extrapolation of the data. Since it is difficult to be certain that the regression equations hold for very short interval durations, T_1 was increased to .5 second which yielded a total duration of 6.75 seconds and a washout detection probability of .64 as shown in Table 6-2.

6.3.3 - Pitch Axis

The situation with regard to downward acceleration in the pitch axis is similar to that of the X-axis with the difference that the velocity limit is not a constraining factor. A washout detection probability of .60 could be obtained with about a 7 second total duration. This would involve an interval 1 duration of about .5 second which is below the minimum value of .75 second studied in experiment 3. This would involve extrapolation from the data and as was done in the case of the Z-axis, this situation was avoided. The interval 1 duration was raised to .75 second resulting in total duration of 6.3 seconds and a washout detection probability of .62 as shown in Table 6-2.

The recommended parameter levels shown in Table 6-2 do not reflect special requirements of specific vehicle simulations. The analysis could be revised based on trade-off considerations for particular simulation cases. In addition, data for numerous other motion cue/washout profiles could be prepared based on the data of Table 6-1. The analysis presented in this section is more an illustration of the application of the data than a basis for firm parameter requirements.

6.4 - Discussion of Results

The data for all axes show a significant dependence on the time interval during which the velocity change is applied. This fact makes the comparison of the current data with previous studies somewhat difficult since threshold values are frequently presented in terms of rate of velocity change without reference to presentation interval. To permit a comparison, it is necessary to assume that the ranges of threshold values from Table 1-1 are valid for presentation intervals greater than about 4.6 seconds since at this duration, the exponential time effect fitted to the current data has little effect. Figure 6-6 shows two curves based on the data of Table 6-1. The regression equations for the translation axes were set equal to .55 and solved for D_x or D_z. A similar procedure was applied to produce .95 D_x or D_z values for all translation motion profiles. These data are shown as a functional relationship between the detection parameter b and the D_x or D_z value necessary for a detection probability of .55 and .95. The horizontal distance between the .55 and .95 curves indicates the range of absolute acceleration level corresponding to the difference between near-chance performance and near certainty of motion detection. For example, the X-axis forward acceleration detection parameter (b) value from Table 6-1 is 1.96. This produces a value of D_x of .0536 for detection probability .55 and 1.1735 for probability .95. The horizontal lines in the upper part of Figure 6-6 show the range of acceleration thresholds reported in Table 1-1.

Figure 6-6 indicates a greater sensitivity to X-axis velocity changes than indicated by the literature. The maximum range interval determined for the current data in the X-axis is that for forward acceleration which ranges from .05 to 1.2 ft/sec^2. Comparison with the range given in Table 1-1 (.4 to 2.6 ft/sec^2) demonstrates that the present data show a lower central value and variability than do the data reported in Table 1-1.

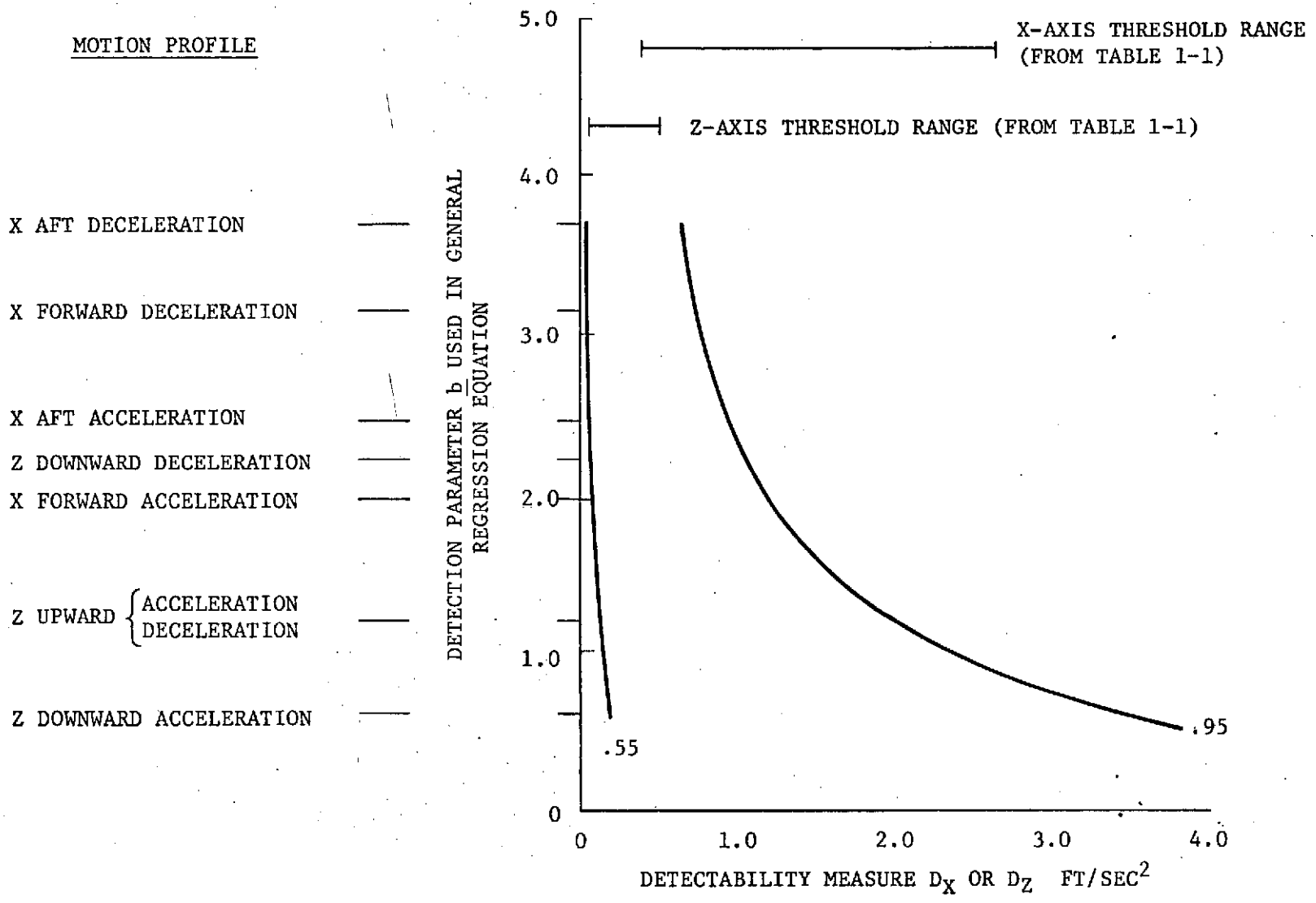

FIGURE 6-6. COMPARISON OF LINEAR ACCELERATION SENSITIVITY FOR CURRENT DATA AND DATA FROM TABLE 1-1

The situation is reversed for the Z-axis data, however. While the .55 probability curve based on the current data falls within the threshold range as given in Table 1-1, the .95 probability curve for Z-axis data rises considerably beyond the upper value based on Table 1-1. It appears likely that the discrepancy arises from the threshold definitions used in earlier work. It does not appear that a threshold definition would produce an acceleration value which would yield 95% accuracy in the present study. The range definition used here includes the acceleration values which produce from .55 to .95 probability of detection. The range of thresholds as given in Table 1-1 should be more strongly constrained not including acceleration values as high as those included in the current .55 to .95 probability range. When this factor is taken into account, the comparison of current data with those from Table 1-1 would appear to indicate that the current data for Z-axis acceleration detection agree fairly well with previous studies. In the case of X-axis detection, however, the current data indicate a greater degree of sensitivity to X-axis acceleration than do the Table 1-1 data.

A second means of comparison, which partly avoids the threshold definition problem, is to substitute Table 1-1 values in the appropriate equations from Table 6-1. The results of this analysis are presented in Table 6-3. It should be noted that these results are based on the assumption that the constraints of presentation time are negligible. Table 6-3 supports the above contention. For the X-axis, substitution of Table 1-1 acceleration values in the present equations yields probabilities ranging from .769 to near unity. This suggests that the current data indicate greater sensitivity to X-axis accelerations than would be supposed based on previous results reported in the literature.

TABLE 6-3 PROBABILITY OF CORRECT DETECTION OF TRANSLATION VELOCITY CHANGE BASED ON SUBSTITUTION OF TABLE 1-1 VALUES IN THE REGRESSION EQUATIONS FROM TABLE 6-1

Axis	Motion Direction	Velocity Change Direction	Threshold Acceleration (ft/sec^2) From Table 1-1		Detection Probability	
			MIN	MAX	MIN	MAX
X	Forward	Acceleration	.394	2.625	.769	.997
X	Aft	Acceleration	.394	2.625	.810	.999
X	Forward	Deceleration	.394	2.625	.855	.999
X	Aft	Deceleration	.394	2.625	.884	.999
Z	Up	Acceleration	.033	.492	.520	.723
Z	Down	Acceleration	.033	.492	.510	.630
Z	Up	Deceleration	.033	.492	.520	.723
Z	Down	Deceleration	.033	.492	.534	.832

The Z-axis data, however, conform more closely to prior results since substitution of Table 1-1 values in the present equations yields probabilities ranging from near-chance performance to a maximum of .832.

As regards angular acceleration in the pitch axis, the relevant data are shown in Figure 6-7. The vertical bar at the top shows threshold range data from Stewart (Ref. 11) for pitch detection. The curves depict the .55 and .95 probability angular accelerations as a function of b. The data show much the same trends as were identified for the Z-axis translation data - the 95% curve being raised considerably relative to the prior data.

The results of substituting the values given by Stewart (Ref. 11) in the appropriate equations from Table 6-1 are shown in Table 6-4. Here the assumption of no presentation time effect is warranted since Stewart's (Ref. 11) data are based on a 10 second presentation interval. Based on this analysis, the current data show fair agreement with Stewart's (Ref. 11) data since detection probabilities in the range from near-chance level to a maximum of .807 are shown in Table 6-4.

A further comparison of the current data with prior data involves individual differences in acceleration/deceleration sensitivity. Stewart (Ref. 11) has noted that large individual differences exist for detection of angular acceleration detection. Clark and Stewart (Ref. 12), however, have shown that pilots and non-pilots do not differ significantly in sensitivity suggesting that the observed individual differences are not strongly influenced by experience in activities reguiring motion cue utilization.

To examine individual difference aspects of the present data, the ratio of between subject variance to total variance was calculated for each axis studied. The relationship required is given by Hayes (Ref. 15) as:

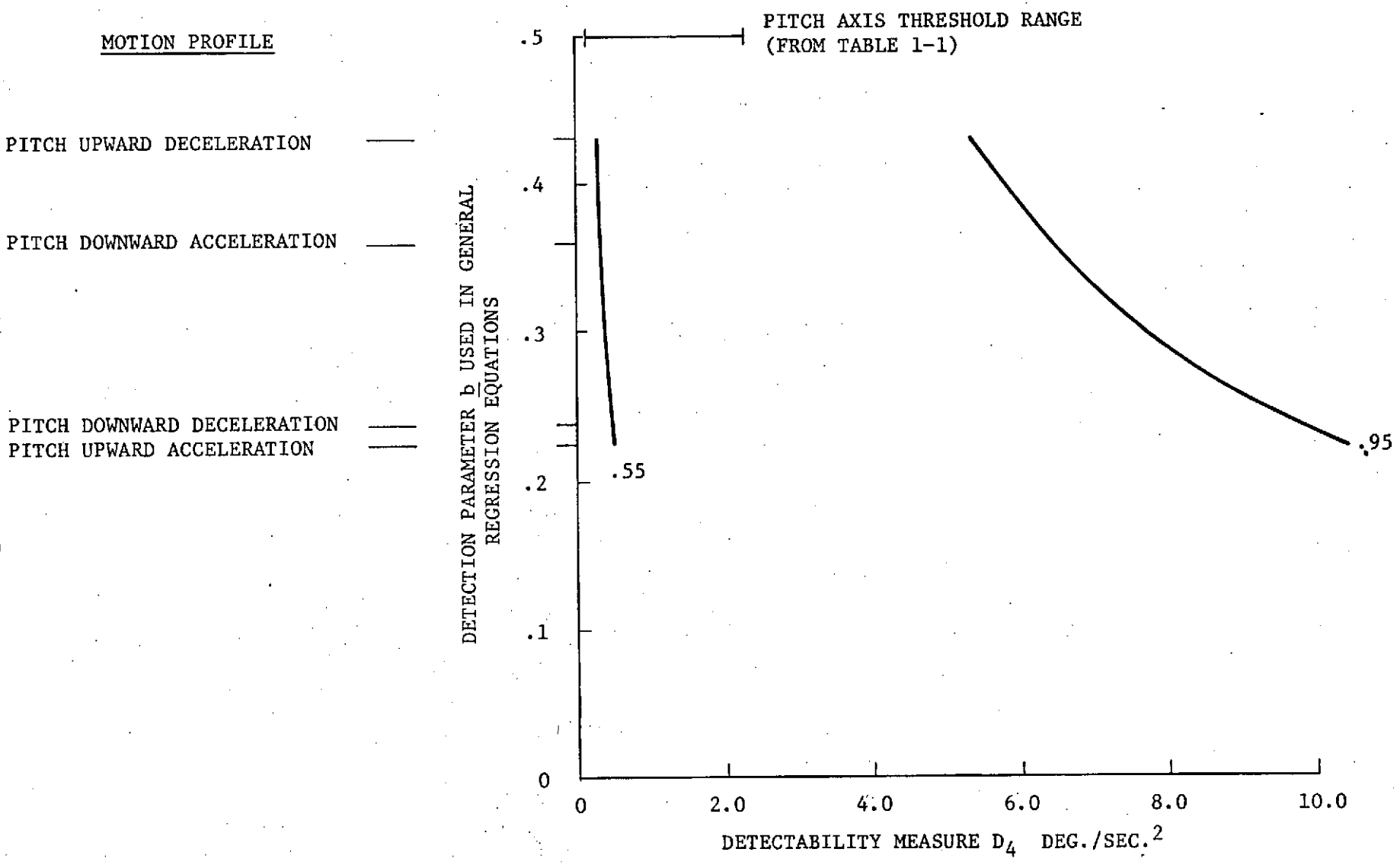

FIGURE 6-7. COMPARISON OF ANGULAR ACCELERATION SENSITIVITY FOR CURRENT DATA AND DATA FROM TABLE 1-1

TABLE 6-4 PROBABILITY OF CORRECT DETECTION OF PITCH VELOCITY CHANGE BASED ON SUBSTITUTION OF STEWART'S (Ref. 11) DATA IN THE REGRESSION EQUATIONS FROM TABLE 6-1

Axis	Motion Direction	Velocity Change Direction	Threshold Acceleration (deg/sec^2) From Table 1-1		Detection Probability	
			MIN	MAX	MIN	MAX
Pitch	Up	Acceleration	.10	2.3	.510	.703
Pitch	Down	Acceleration	.10	2.3	.520	.782
Pitch	Up	Deceleration	.10	2.3	.520	.807
Pitch	Down	Deceleration	.10	2.3	.510	.712

$$W^2 = \frac{\text{SS Between Subjects} - df \cdot \text{MS Within Subjects}}{\text{SS Total} + \text{MS Within}}$$

Where W^2 = the proportion of total variance accounted for by differences between subjects

The appropriate mean squares and the estimates of W^2 are shown in Table 6-5. The data show that approximately 8 percent of the total detection probability variance is accounted for by subject differences in the case of pitch. For the translational axes, however, much lower percentages from 1.3 to 1.6 percent of total variance is associated with differences between subjects. The present data thus suggest that between subjects variation in detecting linear acceleration is less than that for angular acceleration detection.

The hypothesis that contradictory visual motion cues would reduce acceleration sensitivity was tested by the current study with mixed results. The overall detection probabilities for combinations of axis, test condition, motion direction and velocity change direction are illustrated in Figure 6-8. In all cases the visual scene provided cues indicating a forward constant velocity in the X-axis.

In terms of X-axis detection in the forward direction, no effect of test condition is evident. This might be expected since the visual cues did not conflict with non-visual cues - at least as regards direction of motion. For aft motion, however, the reduced sensitivity effect is noted. This effect accounts for the significant interaction of test condition and motion direction.

In the Z-axis, downward acceleration and upward deceleration show some evidence of depressed sensitivity. The remaining conditions appear to produce facilitation of detection. These results cannot be regarded as statistically reliable, however, in view of the lack of a significant three-way interaction.

TABLE 6-5 PROPORTION OF DETECTION PROBABILITY VARIANCE ACCOUNTED FOR BY DIFFERENCES BETWEEN SUBJECTS

Axis	Source	df	SS	MS	W^2
X	Between Subjects	17	5.92	.350	.013
	Within Subjects	1422	231.58	.163	
	TOTAL	1439	237.50	-----	
Y	Between Subjects	6	3.51	.580	.016
	Within Subjects	553	130.06	.235	
	TOTAL	559	133.57	-----	
Pitch	Between Subjects	9	14.70	1.630	.081
	Within Subjects	790	147.89	.187	
	TOTAL	799	162.59	-----	

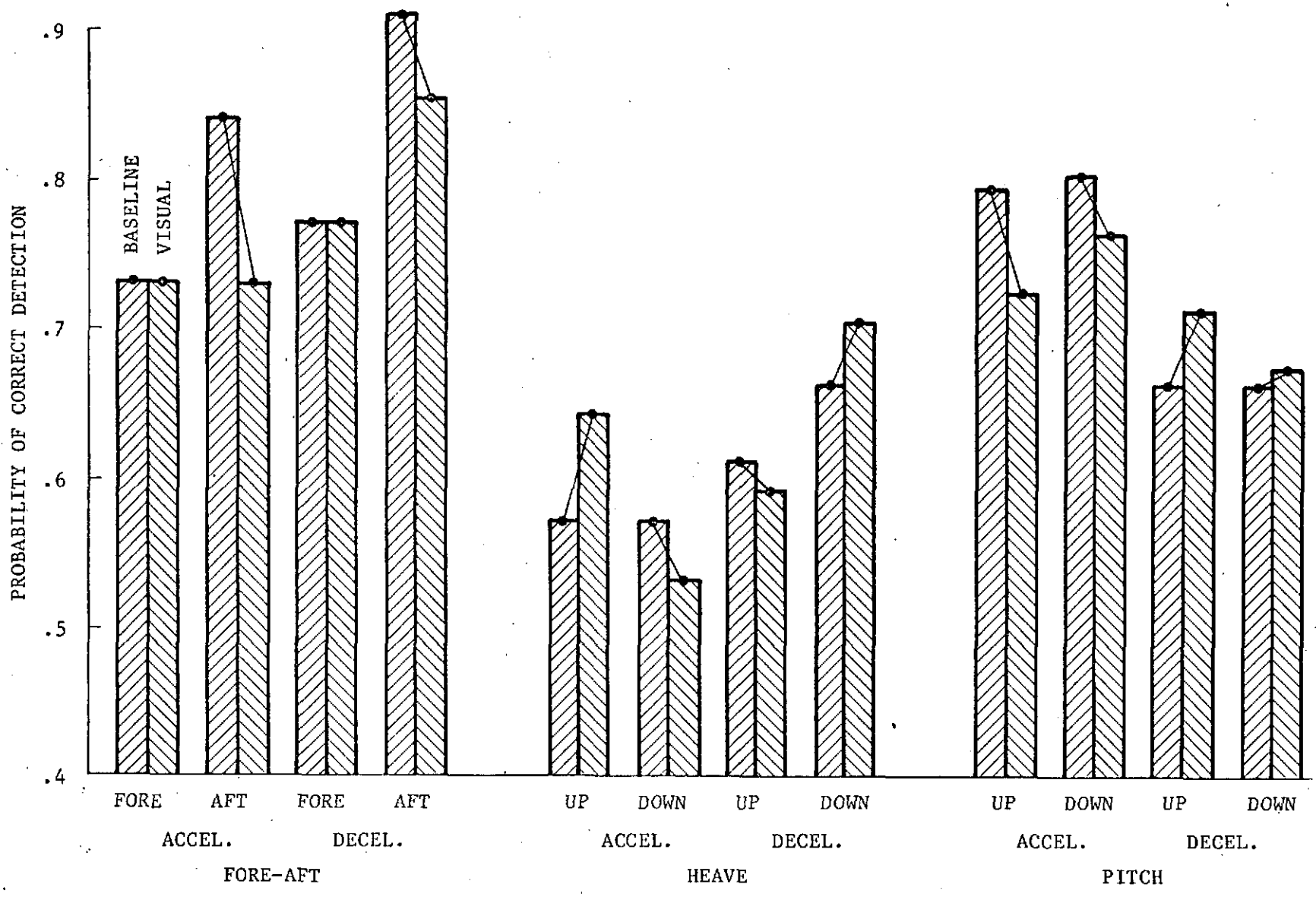

FIGURE 6-8. PROBABILITY OF CORRECT DETECTION OF VELOCITY CHANGE AS A FUNCTION OF AXIS, MOTION DIRECTION, VELOCITY CHANGE DIRECTION, AND TEST CONDITIONS

The pitch data show sensitivity reduction for acceleration but little or no effect for downward deceleration. Upward deceleration appears to produce facilitation. The three-way interaction is not significant for pitch but an interaction between test condition, velocity change direction, and case was found to be significant at the .05 level. This would support an interpretation of sensitivity depression during pitch acceleration but no effect associated with deceleration - the appearance of this trend, however, depending on magnitude of velocity change.

The data then partially support the hypothesis of depression of motion cue sensitivity in response to a contradictory visual presentation for the X and pitch axes. Little evidence of such an effect was found for the Z-axis. It should be noted from Figure 6-8 that the higher probability data points tend to show sensitivity reduction. The Z-axis data may have been obtained too near the chance level for sensitivity depression to occur.

The data suggest that visual effects on non-visual motion sensitivity are worthy of further study. It would appear that since complex vehicle simulation is characterized by control tasks and predominantly forward motion visual cues, somewhat greater acceleration values might be used for washout procedures than would be expected based on studies which remove visual input. Where visual effects on non-visual motion detection were identified in the current data, these effects have been incorporated into the regression equations summarized in Table 6-1.

Finally, it should be noted that the current study made no attempt to isolate vestibular cues from motion cues arising from other sensory modalities. In the translation studies cues involving seat pressure, limb position, and vestibular response were all available to the subject since these would be generally available in simulation exercises. Similarly for the pitch experiment

the center of rotation of the cab was located below the subject's seated position. Translation cues in the X and Z axes were thus confounded with pure rotation cues. For these reasons, the functions presented in Table 6-1 should simply be regarded as empirical regression equations. While an attempt was made to relate the functional forms employed in regression to available information on the vestibular response, it is not implied that the functions used model the vestibular system in any exact way. The functions were developed solely to permit generalization from the data points included in the study.

7.0 EXECUTIVE SUMMARY

The present study deals with motion perception in high fidelity motion simulation. In simulating any of a wide variety of vehicles, methods for providing non-visual motion cues corresponding to vehicle accelerations are of importance. Since a simulator cab will have travel constraints determined by the details of its construction, accelerations commanded by the operator and the resulting rates cannot be maintained indefinitely. An approach being currently considered by persons involved in complex simulation requires approximating the commanded acceleration and then nulling the acquired rate with a deceleration not detectable by the operator. The technique of applying an imperceptible deceleration to null the cab rate is often termed "washout". The maximum rate of velocity change permissible during washout is constrained by the sensitivity of the human observer to non-visual acceleration/deceleration cues. These include the response of the vestibular system, limb position sensors, and pressure sensors in the sensory system.

The study reported here was designed to measure observer sensitivity to accelerations and decelerations using the NASA Marshall Space Flight Center General Purpose Simulator. The objective of the study was to establish acceptable acceleration levels for washout in applying the simulator to a wide variety of vehicles including aircraft, spacecraft, and surface vehicles. Since the General Purpose Simulator utilizes a state-of-the art visual system, the hypothesis was considered that non-visual motion sensitivity would be depressed in the presence of suitable visual cues corresponding to the commanded acceleration and resulting rate. That is, the visual scene presented to the operator need not be washed-out. The visual scene presentation can respond to a commanded acceleration and can continue at the acquired rate

presenting visual cues which correspond to the actual vehicle motion. It is the cab motion which must be washed-out and the washout non-visual cues which should be imperceptible. The visual and non-visual cues are contradictory in this situation and the hypothesis put forth here is that the visual cues will depress sensitivity to the non-visual cues.

To carry out the study, the General Purpose Simulator was programmed to produce cab velocity ramps having various rates of velocity change. Testing was conducted using acceleration and deceleration in both directions in the fore-aft, vertical, and pitch axes. In one trial, motion was presented in only one direction of one axis. During a trial, one interval of time contained constant velocity and one interval contained a velocity ramp. The subject attempted to designate the interval containing a change in velocity. The probability of designating the correct interval was used as the dependent measure.

To test the contradictory cue hypothesis, trial blocks were run under one of two conditions. In the baseline condition, the simulator cab interior was blacked out and the sole task was to respond by designating an interval upon the completion of each trial. In the contradictory cue condition, the subject performed a continuous lateral tracking task with input from the visual system. The visual scene corresponded to a forward constant velocity over a terrain model plus induced lateral excursions which the subject attempted to null via a steering wheel. The cab motion was not influenced by the subject's control actions but was strictly programmed to test non-visual motion cue sensitivity.

The results indicated that detection probability was influenced by all the independent variables in the study which included:

- Axis
- Direction of motion
- Sign of velocity change

- Rate of velocity change
- Interval duration
- Contradictory cues

The contradictory cue hypothesis was partly supported by the data. For X-axis motion, depression of sensitivity was noted for aft motion when contradictory visual cues were introduced. No statistically reliable contradictory cue effects were found for motion in the Z-axis. The pitch data showed sensitivity depression for acceleration but no effect in the case of deceleration.

To generalize the data, a series of exponential regression equations were developed to describe the data and permit interpolation. The regression equations incorporate the effects of rate of change of velocity and interval duration. A separate equation was fitted to the probability data for each combination of axis, motion direction, and direction of velocity change where these variables were found to exert statistically significant effects on detection probability. The resulting regression equations contain a parameter which measures sensitivity to velocity change. These parameter values describe the rate at which probability of detection increases with rate of velocity change and interval duration. Where significant effects of contradictory visual cues were found, these decrements in sensitivity were incorporated into the data fitted by the regression equations.

The resulting equations thus yield a predicted velocity change detection probability for a particular parametric combination of rate of velocity change and the duration over which the rate is applied. This predicted probability can be obtained for any of the three axes studied, and either direction of motion and direction of velocity change.

To illustrate the use of these equations, motion profiles were developed for selected cases where the motion provides a valid acceleration cue and a

washout deceleration which should be imperceptible. The motion profiles were calculated to yield a probability of .90 of proper cue detection and a probability of .60 of washout cue detection (.50 represents the chance level).

Comparison of the present data with other published acceleration threshold data suggested agreement in terms of sensitivity to vertical and pitch axis acceleration. In the case of fore-aft accelerations, however, the present data suggested greater sensitivity than has been reported in the literature.

APPENDIX I

DETECTION OF ACCELERATION/DECELERATION - THEORY

I.1 - The Classical Concept of Threshold

The present discussion examines the consequences of attempts by human observers to detect weak sensory signals. The general concepts developed here apply to a variety of sensitivity experiments. Explicit relations between the theory and the current objectives will be developed in a later section.

Classical studies of the detectability of stimuli employed the notion of the sensory threshold - that stimulus intensity which is "just detectable". Laboratory methods were worked out 100 years ago for obtaining such data. In theory, a well-trained observer should produce an all-or-none step function like curve A in Figure I-1. Unfortunately, empirical functions look more like B.

Due to this fact, an arbitrary convention was adopted. The stimulus value which could be detected with a probability of .50 was taken as the threshold. Today, this approach is still frequently adequate for system design where the intensity of various signals may be selected by the designer and a rough threshold measure is sufficient.

The current purpose, however, is to examine details of detection performance so that arbitrarily chosen thresholds appear inadequate. The naive threshold approach outlined above fails for two reasons - it says nothing about false alarms or cases where the observer reports a signal although none was presented and it does not take account of attitude and motivation factors. In classical psychophysics, it was assumed that the observer was trained to avoid biases and to report his "true mental experience". The presentation of

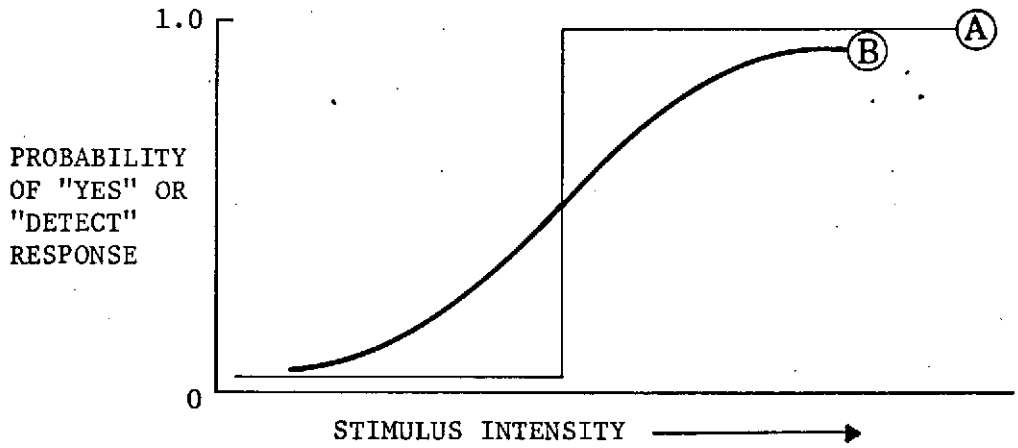

FIGURE I-1. HYPOTHETICAL PSYCHOMETRIC FUNCTIONS

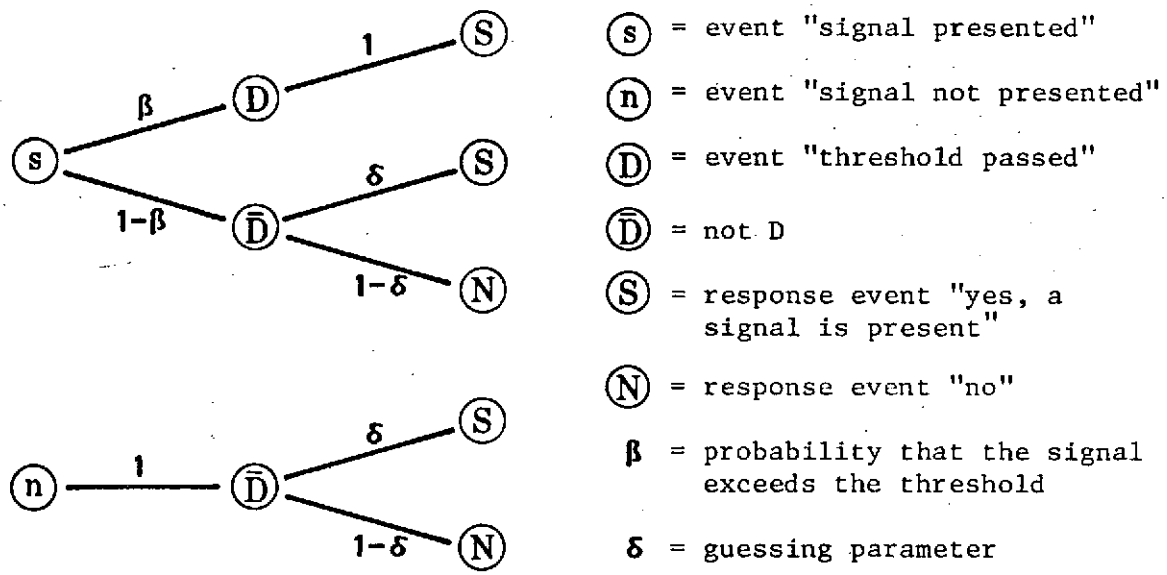

FIGURE I-2. HIGH THRESHOLD THEORY TREE DIAGRAM

experimental trials wherein no signal was presented was referred to as using "catch trials". If an observer reported a detection in these cases, he was told to be more careful. Even so, a certain proportion of false alarm errors were generally found. This led to the correction for guessing model which is sometimes called the high threshold theory today.

I.2 - High Threshold Theory

The theory holds that a somewhat stochastic threshold exists so that a stimulus of fixed intensity has a fixed probability of exceeding the threshold. If the threshold is exceeded, the observer always says "yes". If the threshold is not exceeded, the observer says "yes" with a guessing probability. This probability is a part of the observer's strategy and is influenced by attitudes and motivation. A tree diagram of the process is shown in Figure I-2.

The theory supposes that signals are presented in background noise (in the nervous system if not externally) but that this background can never exceed the threshold so that "true" false alarms can never occur. There are four conditional probabilities:

HIT	$P(S/s) = \beta + (1-\beta)\delta$	If s is present	(I-1)
MISS	$P(N/s) = (1-\beta)(1-\delta)$		
FALSE ALARM	$P(S/n) = \delta$	If s is not present	
CORRECT REJECTION	$P(N/n) = 1-\delta$		

These probabilities may be found empirically. Note that β is a measure of detectability of the signal and δ is a strategy parameter which the observer changes depending on the payoffs and costs of correct responses and errors and on the liklihood of signals. This assumes a detection process which is the reason for this study and a decision process which clouds the issue.

Under the initial problem statement, P(S/s) is of interest for the psychometric function. This statistic, however, is a function of both detection and decision parameters. P(S/s) may increase if the signal detectability (β) is increased or if the observer increases his willingness to guess. The guessing correction approach asserts that β is what should be plotted on the ordinate of the psychometric function. From the model:

$$P(S/s) = \beta + (1-\beta)\, P(S/n) \tag{I-2}$$

$$\beta = \frac{P(S/s) - P(S/n)}{1 - P(S/n)} \tag{I-3}$$

In theory, then, the false alarm rate may be used to "correct" the hit rate for guessing and so estimate the detection parameter β. This approach is still seen in the literature. Unfortunately, the model may be shown to be wrong, as will become apparent shortly. At this point it is sufficient to note that the model predicts that P(S/s) will vary linearly with P(S/n) as the observer changes δ.

I.3 - Theory of Signal Detectability

Much of the motivation for the guessing correction approach derives from the fact that the psychometric function may be displaced along the stimulus intensity axis if changes are inducted in decision behavior. This suggests that a detectability measure is needed which remains invariant when decision behavior varies and which may be estimated from data despite the decision process.

An approach which has been supported by considerable empirical data and which attempts to come to grips with decision factors has been termed the theory of signal detectability (TSD) (Ref. 13). This theory begins by considering

decision processes as an integral part of detection performance rather than tracking it on out of despair as is true of the classical approach.

The point of departure of this theory is a decision axis which may be thought of temporarily as a neural system variable (x) and the probability density functions for sensory effects of noise and signal plus noises. The two distributions are considered to be identical Gaussians. While this assumption is often made, it is not necessary. Empirical results often show non-equality of variances and non-Gaussian forms are sometimes suggested. The result available to the observer on a single trial is a sample value of x. His task is to decide whether this is a sample from the noise alone or the signal plus noise distribution. Formally, if f(x/s) and f(x/n) are the normal densities, and if x is observed, an optimal decision rule involves the likelihood ratio:

$$Lx = \frac{f(x/s)}{f(x/n)} \qquad \text{For single value x} \tag{I-4}$$

Lx therefore has a continuous density over x and we can consider conditional densities for Lx based on noise alone and signal plus noise - f(Lx/n) and f(Lx/s). These densities form the likelihood ratio of the likelihood ratio:

$$L(Lx) = \frac{f(Lx/s)}{f(Lx/n)} \tag{I-5}$$

and it can be shown that

$$L(Lx) = Lx \tag{I-6}$$

So that the decision axis may be considered as a likelihood ratio continuum and neural variables need not be considered. All the information available to

the observer is contained in the likelihood ratio Lx which arose from:

f(Lx/n) If noise alone is present

or

f(Lx/s) If signal plus noise is present

The description of sensory event information as a likelihood ratio dimension is valid even if the sensory event contains multiple cues.

To summarize - TSD rejects the naive threshold assertion and supposes that the observer is continuously sensitive to sensory events. The likelihood ratio captures the information available to him and describes his uncertainty about the source of the observation - noise alone or signal plus noise. If the likelihood ratio were .1, noise would be likely. If 10.0, signal would be likely.

The decision process remains to be postulated. The theory is normative in that it supposes the decision goal to have optimal properties. The postulated process is one familiar in decision theory. It supposes that the observer attempts to maximize expected value.

To express expected value it is necessary to consider the prior signal and noise probabilities and the costs and payoffs associated with the possible outcomes of a trial as shown in Table I-1.

TABLE I-1 - HYPOTHETICAL COST-PAYOFF MATRIX

State Of Stimulus	Response: Noise P(n)	Response: Signal P(s)
Noise	C.R. V(N/n)	F.A. V(S/n)
Signal	MISS V(N/s)	HIT V(S/s)

P(s) = Proportion of trials having signal

P(n) = 1-P(s)

The V entries are values which accrue to the subject based on trial outcome. For example, subjects might be paid 10¢ for a hit and charged 1¢ for a false alarm. In terms of the objective payoff matrix, the expected value of a trial is:

$$EV = P(n)P(N/n)V(N/n) + P(n)P(S/n)V(S/n) + P(s)P(S/s)V(S/s) + P(s)P(S/n)V(S/n) \tag{I-7}$$

It may be shown that EV is maximized within the constraints of the task if a likelihood ratio criterion is used. The criterion is:

$$\text{Say} \quad \left\{ \begin{matrix} S \\ N \end{matrix} \right\} \text{If} \left\{ \begin{matrix} Lx \geq \beta \\ Lx < \beta \end{matrix} \right\} \tag{I-8}$$

Where

$$\beta = \frac{[V(N/n) + V(S/n)]\ P(n)}{[V(S/s) + V(N/s)]\ P(s)} \tag{I-9}$$

The theory is one of an optimal observer who responds "signal" whenever a likelihood ratio as large as or larger than β occurs and who says "noise" otherwise. Data from such an observer yields a particular form of a function called the receiver - operating characteristic. Such a function may be obtained by plotting P(S/s) against P(S/n) as the criterion changes. Suppose that the noise and signal distributions are identical Gaussians which are independent and whose means are separated by σ. Let μ noise = 0 and σ = 1.0. Then the receiver-operating characteristic (ROC) depends on the separation between the noise and signal-to-noise means. In the assumed case or noise = 0 and μ signal + noise = 1.0. The resulting ROC curve has the form shown in Figure I-3.

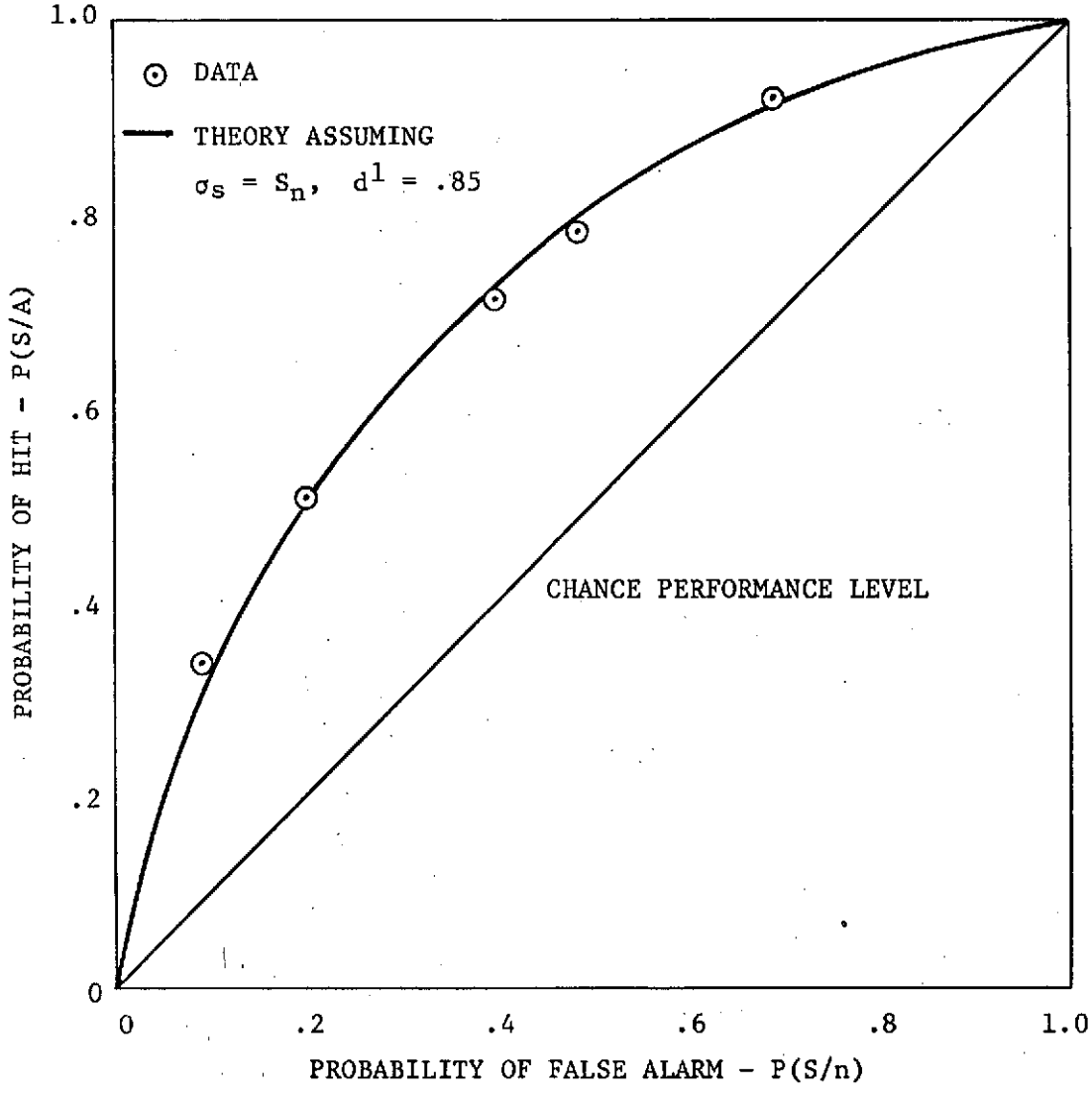

FIGURE I-3. EMPIRICAL RECEIVER OPERATOR CHARACTERISTIC FROM GREEN & SWETS (Ref.13)

The ROC curve predicted by the theory has the following properties:

- The curve is swept out by inducting the observer to vary his criterion.
- The observer moves along the curve based on his decision strategy.
- Changes in detectability sweep out a family of curves. The curve is what is invariable in the situation.
- The curve is symmetrical about the negative diagonal if and only if the noise and signal distributions have identical variance.
- The derivative of the ROC curve gives the likelihood ratio criterion which generated the point in question.
- The area under the ROC curve gives a figure of merit for the detectability of the stimulus which generated the curve.
- For the equal variance case, plotting the ROC curve on double probability paper yields a straight line. From this function a measure d:

$$d^1 = z(S/s) - z(S/n) = \frac{\bar{X}s - \bar{X}n}{\sigma} \qquad \text{(I-10)}$$

may be defined. d^1 is a measure of the separation of the signal and noise distributions. It is calculated operationally from normal transformations of the probability values observed.

I.4 - Empirical Methods for Measuring Signal Detectability

I.4.1 - Yes - No Method

The observer responds yes or no to each trial. A selected proportion of trials contains the signal and the remainder contain noise. This proportion as well as payoffs may be varied to study decision behavior. Signal strength may be varied to study detectability. An example of data from this type of experiment is shown in Figure I-3. The data were collected by Green & Swets (Ref.13) from a task requiring detection of a pure tone in auditory noise.

The yes-no procedure is similar to the psychometric threshold methods previously described. The difference is that the false alarm rate yields as much information on sensory processes as does the hit rate. While the

guessing correction or high threshold model reflects the importance of false alarms, the form of the ROC curve it predicts cannot account for data observed in experiments. We have established that the hit and false alarm probabilities given by the high threshold model are:

$$P(S/s) = \beta + (1-\beta)\delta \qquad \text{(I-11)}$$

$$P(S/n) = \delta \qquad \text{(I-12)}$$

Therefore, substituting eq. (I-12) in eq. (I-11):

$$P(S/s) = \beta + (1-\beta)\,[P(S/n)] \qquad \text{(I-13)}$$

The hit rate is linearly increasing on the false alarm rate as δ varies. Furthermore, the following functional values may be seen to hold:

P(S/n)	P(S/s)
0	β
1	1

The high threshold model ROC curve is <u>linear</u>. It has intercept β and passes through the point (1,1). Application of the two theories to curve fitting using a wide range of empirical data typified by those in Figure I-3 has resulted in rejection of the high threshold theory (Ref. 13).

The problem arising from the application of the theory of signal detectability in the current context is the large number of trials required by the yes-no method. Varying signal strength (magnitude of velocity change in the present case) requires data necessary to plot as many ROC curves as there are signal strength levels of interest. Since 5 to 7 data points are usually necessary to specify one curve, the method is experimentally cumbersome. If

complete ROC data were available, an analysis of parameters of the curve would be performed to characterize the curve and hence to characterize the detectability of a particular level of signal strength. As discussed previously, the parameters used for this purpose are usually d' or the area under the ROC curve. A method called the forced-choice procedure permits estimation of these sensory quantities with one set of empirical data as compared to the yes-no procedure which requires 5 to 7 such data sets. This reduction in experimental effort is accomplished by sacrificing information on the decision criterion adopted by observers under the experimental conditions.

I.4.2 - Forced - Choice Method

In a M-alternative forced-choice method, the observer is presented with M intervals (temporal or spatial). One interval contains a signal and the remainder contain noise alone. The observer attempts to denote the interval containing the signal.

Considering a 2-alternative forced-choice procedure, two observations x_1 and x_2 are available from interval 1 and 2 respectively. This gives rise to two likelihood ratios:

$$Lx_1 = \frac{f(x_1/s)}{f(x_1/n)} \quad \text{and} \quad Lx_2 = \frac{f(x_2/s)}{f(x_2/n)} \tag{I-14}$$

The assumed decision rule is that the observer endorses the interval having the higher likelihood ratio. That is:

$$\text{Say} \begin{cases} \text{Interval 1} \\ \text{Interval 2} \end{cases} \quad \text{If} \begin{cases} Lx_1 > Lx_2 \\ Lx_2 > Lx_1 \end{cases} \tag{I-15}$$

The dependent measure generally employed in forced-choice experiments is the probability of correct.

Notice that of the two likelihood ratios Lx_1 and Lx_2, one arose from the signal plus noise distribution and one arose from the noise distribution. The possible single trial outcomes are shown in Table I-2:

TABLE I-2 - FORCED CHOICE PROCEDURE SINGLE TRIAL OUTCOMES

Case	Interval 1	Interval 2	Likelihood Ratio Relation	Interval Endorsed	Result
1	Signal	Noise	$Lx_1 > Lx_2$	1	Correct
2	Signal	Noise	$Lx_1 > Lx_2$	2	Error
3	Noise	Signal	$Lx_1 > Lx_2$	1	Error
4	Noise	Signal	$Lx_1 > Lx_2$	2	Correct

Under the cases where the signal is present in the first interval, suppose that $Lx_2 = L$, then the probability of correct equals the probability that $Lx_1 > L$. Considering any value of L:

$$P(C \curvearrowright Lx_2 = L) = P(Lx_2 = L)\, P(Lx_1 > L) \qquad \text{(I-16)}$$

The second term - $P(Lx_1 > L)$ - is the area under the distribution of Lx given signal from L to $+\infty$:

$$P(Lx_1 > L) = \int_L^{+\infty} f(Lx/s)\, dLx \qquad \text{(I-17)}$$

Now suppose that in the yes/no procedure, the observer adopts a criterion likelihood ratio (β) equal to L. Then by the yes/no response axiom:

$$P_1(S/s) = \int_L^{+\infty} f(Lx/s)dLx \qquad \text{(I-18)}$$

So that:

$$P(x \cap Lx_2 = L) = P(Lx_2 = L)\ PL(S/s) \qquad \text{(I-19)}$$

The total probability - P(C) - is the sum of joint values $P(C \cap Lx_2 = L)$ over all values of L:

$$P(C) = \int_{-\infty}^{+\infty} P(Lx_2 = L)\ P(Lx_1 > L)dL \qquad \text{(I-20)}$$

$$= \int_{-\infty}^{+\infty} P(Lx_1 > L) \quad \int_L^{\infty} f(Lx/s)dLx \quad dL \qquad \text{(I-21)}$$

Green and Swets (Ref.13) have shown that the right hand side of this expression depends entirely on parameters of the yes-no ROC curve in such a way that by a change in the variable of integration:

$$P(C) = \int_0^1 [1 - P(S/n)]dP(S/s) \qquad \text{(I-22)}$$

So that the probability of correct in a two-alternative forced-choice task is, in theory equal to the area under the yes-no ROC curve. Green and Swets (Ref.13) have summarized considerable evidence showing that this result does hold for empirical data. In fact one of the strong points of the theory is the demonstrated independence of the sensory measures of the experimental method employed.

In summary, then, the initial problem was to specify a method for acceleration sensitivity measurement which would be independent of changes in decision behavior. The theory of signal detectability has been shown to account for

numerous experimental findings and, according to the theory, the probability of correct in a two-alternative forced-choice task will be equal to the area under the yes-no ROC curve and therefore free of effects of observer decision factors. Accordingly, the forced-choice method was selected for use in the current study. Signals were defined to consist of a constant acceleration/velocity ramp presented during either the first or second of two fixed duration temporal intervals. The subject's task was to report which interval he judged to contain a change in velocity.

References

1. Conrad, B.; Dourvillier, J.G.; and Schmidt, S.F. Washout Circuit Design for Multidegree-of-Freedom Moving Base Simulators. Paper presented at AIAA Visual and Motion Simulation Conference. NASA Ames Research Center, Moffett Field, California, Sept. 1973.

2. Parrish, R.V.; Dieudonne, J.E.; Bowles, R.L.; and Martin, D.J. Coordinated Adaptive Washout for Motion Simulators. Paper presented at AIAA Visual and Motion Simulation Conference. NASA Ames Research Center, Moffett Field, California, Sept. 1973.

3. Huddleston, H.F. Cockpit Motion Requirements for Flight Simulation.

4. Fogel, L.J. Biotechnology, Prentice-Hall, Englewood Cliffs, N.J., 1973.

5. Clark, B. and Graybiel, A. Linear acceleration and deceleration as factors influencing nonvisual orientation during flight. J. Aviation Med., 1949, 20, 92-101.

6. Walsh, E.G. J. Physiol., 1961, 155, 506-513.

7. Gurnee, H. J. Exp. Psychol., 1934, 17, 270-285.

8. Jongkees, L.B.W. and Groen, J.J. The nature of the vestibular stimulus. J. Laryngol. Otol., 1946, 61, 529-541.

9. Jones, M. and Young, L.R. Directional uncertainty during vertical acceleration. Aerospace Medicine, 1974 - in preparation.

10. Jones, G.M.; Barry, W.; and Kowalsky, N. Aerospace Medicine, 1964, 35, 984-989.

11. Stewart, J.D. Human perception of angular acceleration and implications in motion simulation. Journal of Aircraft, 1971, 8, 4, 248-253.

12. Clark, B. and Stewart, J.D. Comparison of the sensitivity to rotation of pilots and nonpilots. Aerospace Medicine, 1972, 43, 1, 8-12.

13. Green, D.M. and Swets, J.A. Signal Detection Theory and Psychophysics, John Wiley & Sons, Inc., 1966.

14. Guedry, F.E., Jr. Psychophysiological studies of vestibular function.

15. Hayes, W.L. Statistics, Holt, Rinehart and Winston, 1963.